

ONE AND TWO IMPULSE RENDEZVOUS TRAJECTORIES
FOR SPACE SHUTTLE PAYLOAD
RETRIEVAL OPERATIONS

by

Ronald Lafe Farris, B.S.

THESIS

Presented to the Faculty of the Graduate School of

The University of Texas at Austin

in Partial Fulfillment

of the Requirements

for the Degree of

MASTER OF SCIENCE IN ENGINEERING

THE UNIVERSITY OF TEXAS AT AUSTIN

May 1978

ONE AND TWO IMPULSE RENDEZVOUS TRAJECTORIES
FOR SPACE SHUTTLE PAYLOAD
RETRIEVAL OPERATIONS

APPROVED:

Wallace J. Fowler

Byron D. Tapley

ONE AND TWO IMPULSE RENDEZVOUS TRAJECTORIES
FOR SPACE SHUTTLE PAYLOAD
RETRIEVAL OPERATIONS

by

Ronald Lafe Farris, B.S.

THESIS

Presented to the Faculty of the Graduate School of
The University of Texas at Austin
in Partial Fulfillment
of the Requirements
for the Degree of

MASTER OF SCIENCE IN ENGINEERING

THE UNIVERSITY OF TEXAS AT AUSTIN

May 1978

ACKNOWLEDGEMENTS

I wish to thank Dr. Wallace T. Fowler for his initial encouragement to enter graduate school and for his continued interest and assistance throughout my academic career.

Also, I especially thank my loving wife, Barbara, for her unending faith and support during the writing of this thesis. Between critiquing the rough drafts and typing this final revision, she has probably devoted as much of her time to this project as I have.

Finally, I would like to express my deepest appreciation to my wonderful parents, Jack and Ruth Farris, for their love and guidance throughout my life and for making it possible for me to attend this university.

Thesis submitted to Committee on April 17, 1978

TABLE OF CONTENTS

	Page
Acknowledgments	iii
CHAPTER 1 Introduction	1
CHAPTER 2 Coordinate System and Derivation of Equations	7
CHAPTER 3 Two Impulse Rendezvous Trajectories	13
CHAPTER 4 One Impulse Rendezvous Trajectories	33
CHAPTER 5 Generalized Rendezvous Techniques	39
CHAPTER 6 Trajectory Optimization	61
CHAPTER 7 Conclusions and Recommendations	74
References	81
Vita	

CHAPTER 1

Introduction

As the space shuttle becomes operational in the early 1980's, two of its primary functions will be the deployment of new payloads to pre-specified orbits and the retrieval of objects already in space. Ultimately, it may be used to repair or replace satellites which have malfunctioned. A possible scenario for such a mission involves an initial orbital transfer by the shuttle to a location in the vicinity (about 1000 ft) of the satellite to be retrieved and repaired. This location is called a Stationkeeping Point and allows the crew to visually inspect the satellite and to make systems checks before final rendezvous maneuvers are initiated. The final rendezvous and all shuttle attitude changes employ the Reaction Control System (RCS) or the Vernier Reaction Control System (VRCS) to produce all necessary changes in the linear and angular velocities of the shuttle. The RCS is composed of 38 strategically located 870 lbf rocket thrusters. The VRCS has six thrusters, each capable of producing 25 lbf.

The final rendezvous maneuver is designed to place the shuttle within 50 ft of the satellite so that it can be grappled. The relative velocity at the end of the final approach must be small enough so that the Remote Manipulator System (RMS) may be used to effect a capture. Upon retrieval and repair (or replacement), the satellite is deployed

with the RMS. A trajectory is then initiated which will return the shuttle to the stationkeeping point. From this location, the satellite may be tested in insure proper operation. Next, an orbital transfer may be computed for approach to another satellite or for reentry and landing.

For ease of discussion, two mission phases have been defined which encompass the above maneuvers. Proximity Operations denotes that phase of the mission when the shuttle is either at the stationkeeping point or in transit to or from the satellite. The Payload Handling phase occurs at any time when the shuttle is within the RMS capture range (50 ft) of the satellite and is actively involved in a capture or deployment procedure.

There are four primary constraints which govern the motion of the shuttle during the payload handling and proximity operations phases of the mission. These are:

- (1) RMS constraints
- (2) Plume impingement constraints
- (3) Safety constraints
- (4) Propellant constraints

The RMS is mainly composed of a 50 foot, anthropomorphic, remotely operated mechanical arm which is used to stow or deploy satellites (or any payload) to or from the shuttle cargo bay. The structural design limits of the unloaded manipulator arm impose a maximum tip velocity of 2.0 fps during any retrieval or deploying operation. However, for a maximum payload of 65000 lb, the allowable translation rate is reduced to 0.2 fps. That is, if the relative velocity between the shut-

tle and a 65000 lb payload is greater than 0.2 fps while the payload is being held by the RMS, then possible structural damage may occur within the arm mechanism. Thus, any rendezvous trajectory to a large payload is constrained to have a final closure rate of less than 0.2 fps.

The second constraint is that of plume impingement on the satellite due to the space shuttle thrusters. Plume impingement occurs when the exhaust particles (burned propellant) from the shuttle RCS thrusters strike the satellite. At close distances, these particles can exert sufficient force on the satellite so as to cause it to tumble out of control. Also, the particles may cause damage to delicate instruments which may be aboard the satellite. The plume, or envelope of exhaust particles, has been shown in JSC-12976¹ to expand radially for distances of about 500 ft at angles exceeding 90° perpendicular to the centerline of the thruster nozzle.

Safety constraints have been imposed by NASA and specify that all retrieval trajectories must allow the mission specialist astronaut to view the target body at all times during the final rendezvous.

The last constraint is imposed by the fact that the available RCS fuel must be allocated among a number of maneuvers which must be completed on a given shuttle mission. Therefore, it is reasonable to require that minimum amount of fuel be consumed in each rendezvous procedure.

Hence, the problem becomes one of approaching a predetermined target point in space (satellite location) with a rendezvous trajectory which:

- (1) has a final relative velocity of less than 0.2 fps,
- (2) does not require an initial or final braking thrust which will cause plume impingement,
- (3) allows astronauts to visually track the target vehicle, and
- (4) uses a minimum of fuel.

This study discusses the above problem and outlines several possible solutions. Conclusions are drawn and recommendations are made concerning an optimal solution. The following assumptions have been made to simplify the presentation.

- (1) The rendezvous trajectories presented are assumed to have started at a location in the vicinity of the target point. This initial position is called a stationkeeping point. An analysis of the space shuttle motion prior to attaining the stationkeeping point is not presented.
- (2) An inverse square gravitational field with no perturbing forces is assumed.
- (3) The satellite to be retrieved (or target point for deploying) is assumed to be in a very nearly circular orbit.
- (4) Only in-plane motion will be considered, i.e., all rendezvous trajectories will remain in the orbital plane of the target point. This corresponds to the X-Y plane of the coordinate system to be described in Chapter 2.
- (5) It is assumed that accurate range and range-rate data of the target point with respect to the shuttle are available to the crew during the proximity operations mission phase.

The assumption that all trajectories originate from a nearby stationkeeping point is realistic since NASA would like such an opportunity to observe the satellite or body of interest and make shuttle systems checks before the final rendezvous procedure is begun.

The assumption of two body motion is justified due to the short rendezvous times involved. Also, because of the small distances involved, any perturbing forces which are present will affect both bodies equally.

The assumption of circular orbits is made for clarity of presentation and comprehension of graphical simulation results only. The equations outlined in Chapter 2, as well as all computer programs developed for analysis, are independent of eccentricity.

It has been shown by D. D. Mueller² that the out-of-plane motion of an orbiting body is nearly independent of in-plane motion for distances of several kilometers. This leads to the fourth assumption which was made. For the case of an out-of-plane stationkeeping point, the shuttle need only wait until it passes through the orbital plane of the target body. At this point, the shuttle would thrust to reduce its out-of-plane velocity component to zero.

The fifth assumption is made since approaches to within 50 ft of the target point are to be made from stationkeeping distances approaching 1000 ft. Accurate range rate data is necessary to insure that the initial relative velocity is zero, i.e., the space shuttle is in a stationkeeping position.

The overall study will consist of the definition of a coordinate system and a formulation of the equations of motion which govern all shuttle motion. Using these equations, methods will be developed to identify specific one and two impulse rendezvous trajectories. A general technique will be outlined for rendezvous from any position in the vicinity of the target point. Also, a rendezvous method will be developed to simulate the line-of-sight trajectories currently under study by NASA. Rendezvous trajectories from prime stationkeeping locations will be simulated using all techniques. Those trajectories which satisfy all imposed constraints will then be presented and compared in order to find an optimal solution.

CHAPTER 2

Definition of Coordinate System and Derivation of Equations

A non-inertial coordinate system is defined and used in the derivation of the equations of relative shuttle motion. The origin of this system is assumed to be the target point for all shuttle rendezvous trajectories. In the following discussion of coordinate system parameters, the origin will be referred to as the "target" and subscripted as such.

The positive Y axis of our coordinate system is chosen to be in the orbital plane and directed away from the earth. The positive Z axis is set parallel to the angular momentum vector of the orbit and in the same direction. The requirement of a right handed system fixes the X axis to be colinear with the velocity vector of the rendezvous target; however, they are opposite in sign. This coordinate system is shown in Figure 1, where $\vec{V}_{T/E}$ is the velocity of the origin (target) with respect to the earth; $\vec{R}_{S/T}$, the position of the shuttle relative to the target; $\vec{R}_{S/E}$, the position of the shuttle relative to the center of the earth; $\vec{R}_{T/E}$, the position of the target relative to the center of the earth; ψ , the attitude angle of the target; and v , the true anomaly of the target point.

With the above coordinate system in mind, the Lagrangian formulation has been used to derive the equations of relative motion. In

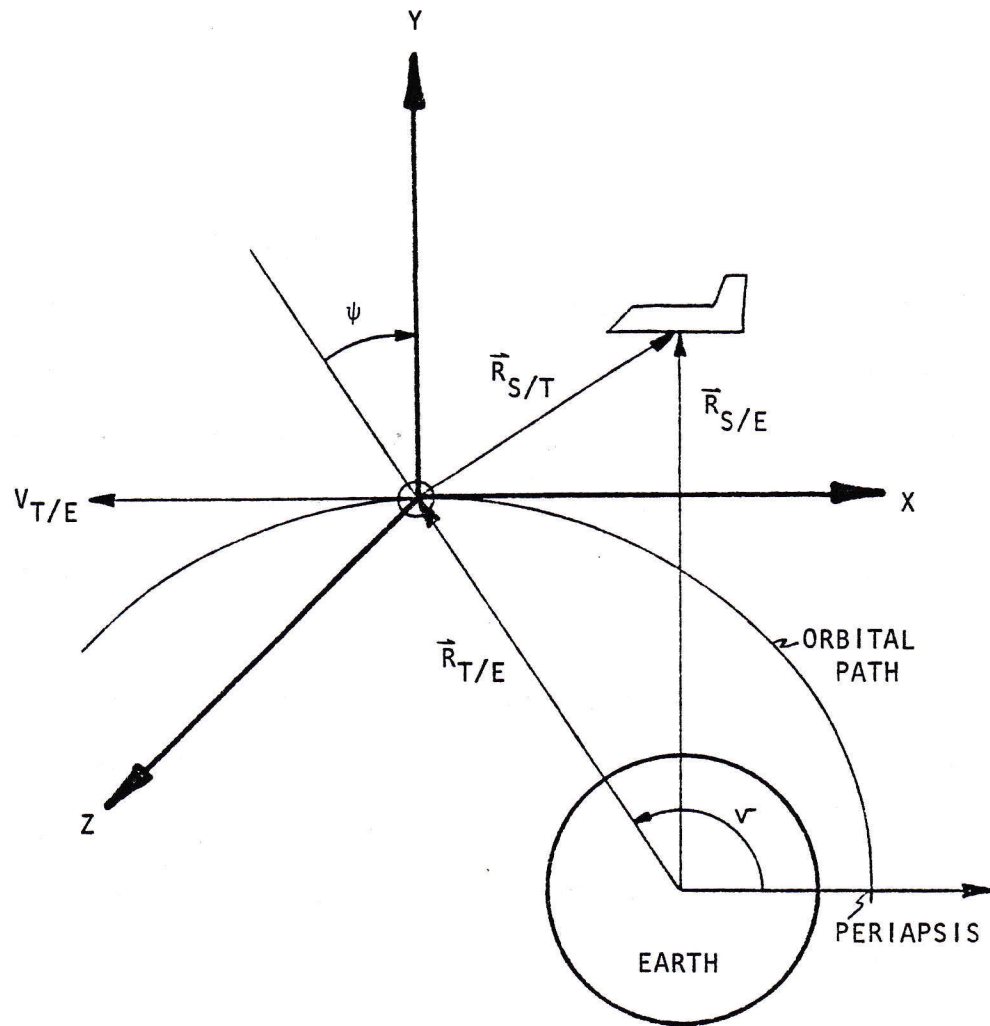


Figure 1 Target Point Centered Coordinates

forming the Lagrangian

$$L = T - V \quad (1)$$

the kinetic energy, T , and the potential energy, V , must be computed.

The potential energy in this case takes the familiar form

$$V = \frac{-G(M \cdot m)}{R} \quad (2)$$

where m is the mass of the orbiting body; M , the mass of the central body; R , the distance between the centers of mass of the two bodies; and G , the universal gravitational constant. Conventially, GM is replaced by μ , the gravitational parameter for the specific central body. Thus, the potential energy to be used in Eq. (1) is

$$V = - \frac{\mu m}{R} \quad (3)$$

The Kinetic energy,

$$T = \frac{1}{2} mV^2 \quad (4)$$

lacks only an expression of V (the inertial velocity of the orbiting mass) in the noninertial reference frame just described. The inertial frame is assumed to be fixed at the center of the earth. This assumption makes the necessary transformation of T and V into the orbiting reference frame much simpler.

The orbiting mass of interest in this case is the space shuttle. As discussed, the noninertial frame is assumed to orbit the earth as if it were fixed to the target vehicle. As shown in Figure 1 then,

$R = |\vec{R}_{S/E}|$, and

$$\vec{R}_{S/E} = \vec{R}_{T/E} + \vec{R}_{S/T} \quad (5)$$

from figure 1 it can be seen that if

$$r_T = |\vec{R}_{T/E}|$$

then $\vec{R}_{T/E}$ can be written in the noninertial frame as

$$\vec{R}_{T/E} = r_T (-\vec{i} \sin\psi + \vec{j} \cos\psi), \quad (6)$$

where \vec{i} and \vec{j} are unit vectors in the rotating frame and ψ is the angle between the noninertial Y axis and $\vec{R}_{T/E}$, positive clockwise as shown in the figure. $\vec{R}_{S/T}$ may be separated into components as

$$\vec{R}_{S/T} = X\vec{i} + Y\vec{j} + Z\vec{k}, \quad (7)$$

so $\vec{R}_{S/E}$ becomes

$$\vec{R}_{S/E} = (X - r_T \sin\psi)\vec{i} + (Y + r_T \cos\psi)\vec{j} + Z\vec{k}. \quad (8)$$

Since $R = |\vec{R}_{S/E}| = (\vec{R}_{S/E} \cdot \vec{R}_{S/E})^{1/2}$, the potential energy can be written as

$$V = \frac{-\mu}{(X - r_T \sin\psi)^2 + (Y + r_T \cos\psi)^2 + Z^2} \quad (9)$$

In the kinetic energy equation, (4), the element that must be transformed is V^2 , the square of the inertial velocity. This is done by noting that the inertial velocity of the shuttle, $\vec{V}_{S/E}$ may be written

$$\vec{V}_{S/E} = \frac{d}{dt} \vec{R}_{S/E} \Big|_I = \frac{d}{dt} \vec{R}_{S/E} \Big|_R + \vec{\omega}_{T/E} \times \vec{R}_{S/E}, \quad (10)$$

where $\frac{d}{dt} \vec{R}_{S/E} \Big|_I$ is the time derivative of $\vec{R}_{S/E}$ in the inertial frame,

$\frac{d}{dt} \vec{R}_{S/E} \Big|_R$ is its time derivative in the rotating frame, and $\vec{\omega}_{T/E}$ is the

angular velocity of the rotating frame. The magnitude of the angular velocity vector, $\vec{\omega}_{T/E}$, is the difference of the angular velocity, \dot{r} , of the target position vector from the center of the earth, $\vec{R}_{T/E}$, and the rate of change of the target attitude angle, $\dot{\psi}$. The direction of $\vec{\omega}_{T/E}$ is, by definition of the reference frame, the same as that of the Z axis. Thus,

$$\vec{\omega}_{T/E} = (\dot{r} - \dot{\psi})\vec{k}. \quad (11)$$

Substituting Eq. (5) into (10) yields

$$\vec{v}_{S/E} = \frac{d}{dt} (\vec{R}_{T/E} + \vec{R}_{S/T}) \Big|_R + \vec{\omega}_{T/E} \times (\vec{R}_{T/E} + \vec{R}_{S/T}) \quad (12)$$

Observing Eqs. (6) and (7) and performing the indicated operations in Eq. (12) result in the following expressions for the terms on the right

$$\begin{aligned} \frac{d}{dt} \vec{R}_{T/E} \Big|_R &= \dot{r}_T (-\vec{i} \sin\psi + \vec{j} \cos\psi) + r_T (-\dot{\psi} \cos\psi - \dot{\psi} \sin\psi) \\ &= -(\dot{r}_T \sin\psi + r_T \dot{\psi} \cos\psi) \vec{i} + (\dot{r}_T \cos\psi - r_T \dot{\psi} \sin\psi) \vec{j} \end{aligned} \quad (13)$$

$$\frac{d}{dt} \vec{R}_{S/T} \Big|_R = \dot{X} \vec{i} + \dot{Y} \vec{j} + \dot{Z} \vec{k} \quad (14)$$

$$\vec{\omega}_{T/E} \times \vec{R}_{T/E} = [-r_T (\dot{\nu} - \dot{\psi}) \cos\psi] \vec{i} + [-r_T (\dot{\nu} - \dot{\psi}) \sin\psi] \vec{j} \quad (15)$$

$$\vec{\omega}_{T/E} \times \vec{R}_{S/T} = -Y (\dot{\nu} - \dot{\psi}) \vec{i} + X (\dot{\nu} - \dot{\psi}) \vec{j} \quad (16)$$

Adding Eqs. (13), (14), (15), and (16) yields

$$\begin{aligned} \vec{v}_{S/E} &= [\dot{X} - Y (\dot{\nu} - \dot{\psi}) - r_T \dot{\nu} \cos\psi - \dot{r}_T \sin\psi] \vec{i} \\ &\quad + [\dot{Y} + X (\dot{\nu} - \dot{\psi}) - r_T \dot{\nu} \sin\psi + \dot{r}_T \cos\psi] \vec{j} + \dot{Z} \vec{k}, \end{aligned} \quad (17)$$

and

$$\begin{aligned} v_{S/E}^2 &= \vec{v}_{S/E} \cdot \vec{v}_{S/E} = [\dot{X} - Y (\dot{\nu} - \dot{\psi}) - r_T \dot{\nu} \cos\psi - \dot{r}_T \sin\psi]^2 \\ &\quad + [\dot{Y} + X (\dot{\nu} - \dot{\psi}) - r_T \dot{\nu} \sin\psi + \dot{r}_T \cos\psi]^2 + \dot{Z}^2 \end{aligned} \quad (18)$$

Substituting this into the relation for kinetic energy, Eq. (4), and then substituting the result and Eq. (9) (the potential energy) in Eq. (1), shows the Lagrangian to have the form

$$\begin{aligned} L &= \frac{1}{2} m [\dot{X} - Y (\dot{\nu} - \dot{\psi}) - r_T \dot{\nu} \cos\psi - \dot{r}_T \sin\psi]^2 \\ &\quad + [\dot{Y} + X (\dot{\nu} - \dot{\psi}) - r_T \dot{\nu} \sin\psi + \dot{r}_T \cos\psi]^2 + \dot{Z}^2 \end{aligned} \quad (19)$$

$$+ \frac{m g r_T^2}{[(X + r_T \sin\psi)^2 + (Y + r_T \cos\psi)^2 + Z^2]^{1/2}} \quad (19 \text{ cont})$$

from this, using X , Y , and Z as the generalized coordinates, Lagrangian analysis produces the equations of motion as

$$\begin{aligned} \ddot{X} = & 2\dot{Y}(\dot{v}-\dot{\psi}) + Y(\ddot{v}-\ddot{\psi}) + X(\dot{v}-\dot{\psi}) + (2\dot{r}_T\dot{v} + r_T\ddot{v})\cos\psi \\ & + (\ddot{r}_T - r_T\dot{v}^2)\sin\psi - \frac{\mu(X-r_T\sin\psi)}{[(X-r_T\sin\psi)^2 + (Y+r_T\cos\psi)^2 + Z^2]^{3/2}} \end{aligned} \quad (20a)$$

$$\begin{aligned} \ddot{Y} = & -2\dot{X}(\dot{v}-\dot{\psi}) - X(\ddot{v}-\ddot{\psi}) + Y(\dot{v}-\dot{\psi})^2 + (2\dot{r}_T\dot{v} + r_T\ddot{v})\sin\psi \\ & + \frac{\mu(Y+r_T\cos\psi)}{[(X-r_T\sin\psi)^2 + (Y+r_T\cos\psi)^2 + Z^2]^{3/2}} \end{aligned} \quad (20b)$$

$$\ddot{Z} = \frac{-\mu Z}{[(X-r_T\sin\psi)^2 + (Y+r_T\cos\psi)^2 + Z^2]^{3/2}} \quad (20c)$$

These equations may be further simplified when the circular orbit assumption is introduced. In this case, ψ , $\dot{\psi}$, and $\ddot{\psi}$ are identically zero since the Y axis is always directed radially away from the center of the earth.

The form of the equations of motion derived in this way is not readily susceptible to analytic solution but can be dealt with using numerical techniques. The results of this numerical integration method are described in the following chapters.

CHAPTER 3

Two Impulse Rendezvous Trajectories

The problem of traveling from one point to another point in space on a trajectory with pre-specified initial and final velocities is a two point boundary value problem. The two-impulse rendezvous trajectories which are being considered fall under this classification. Since the two point boundary value problem cannot be solved in closed form, the problem must be restated as an initial value problem. Thus, if the location of a body (shuttle) in space at a given time is known, along with the direction and magnitude of its velocity at that time, its position and velocity at any other time may be calculated via numerical integration of the equations of motion.

The trajectory analysis may be transformed to an initial value problem by simply letting the target position (satellite location) and the desired relative velocity of the shuttle at the point (final closure velocity before the second impulse) be the initial conditions which are required. Then, by integrating backwards in time, the prior trajectory (both position and velocity) of the shuttle may be determined. In actual practice, any point along this prior trajectory may be chosen as an initial location or stationkeeping point from which to initiate rendezvous. The velocity indicated at any such position by the negative time integration procedure will then be the velocity which is required

to effect a rendezvous. The final closure rate of any such rendezvous trajectory will be identical to the initial velocity used for the negative time integration. If this final closure rate is greater than 0.2 fps, it must be reduced to 0.2 fps or less (RMS capture constraint) by using the RCS or VRCS thrusters. This thrust would complete a two impulse rendezvous.

A discussion of stationkeeping points is in order at this time. Due to a decrease in orbital velocity with an increase in orbital altitude, the distance between two points in space will not remain constant unless they are close to each other and at the same orbital altitude. For this reason, the only stable stationkeeping points for the shuttle would be points directly forward of or behind the target body. This would be any point on the X axis of the coordinate system as defined earlier.

It should also be noted that the optimum viewing area for the mission specialist astronaut is directly above and to the rear of the shuttle. Thus, the apparent motion of the target body during an optimum rendezvous trajectory will bring it down, over the shuttle tail, and above the cargo bay area of the shuttle where it will be captured by the RMS.

The negative time integration procedure was used to generate a series of trajectories by varying both the magnitudes and directions of the initial velocities. Initial velocities (\vec{V}_0) in each of eight directions, as indicated by Figure 2, were tested. Three initial velocity magnitudes were specified for each of these directions. The velocities chosen were 0.5 fps, 1.0 fps, and 1.5 fps. The orbit of the origin

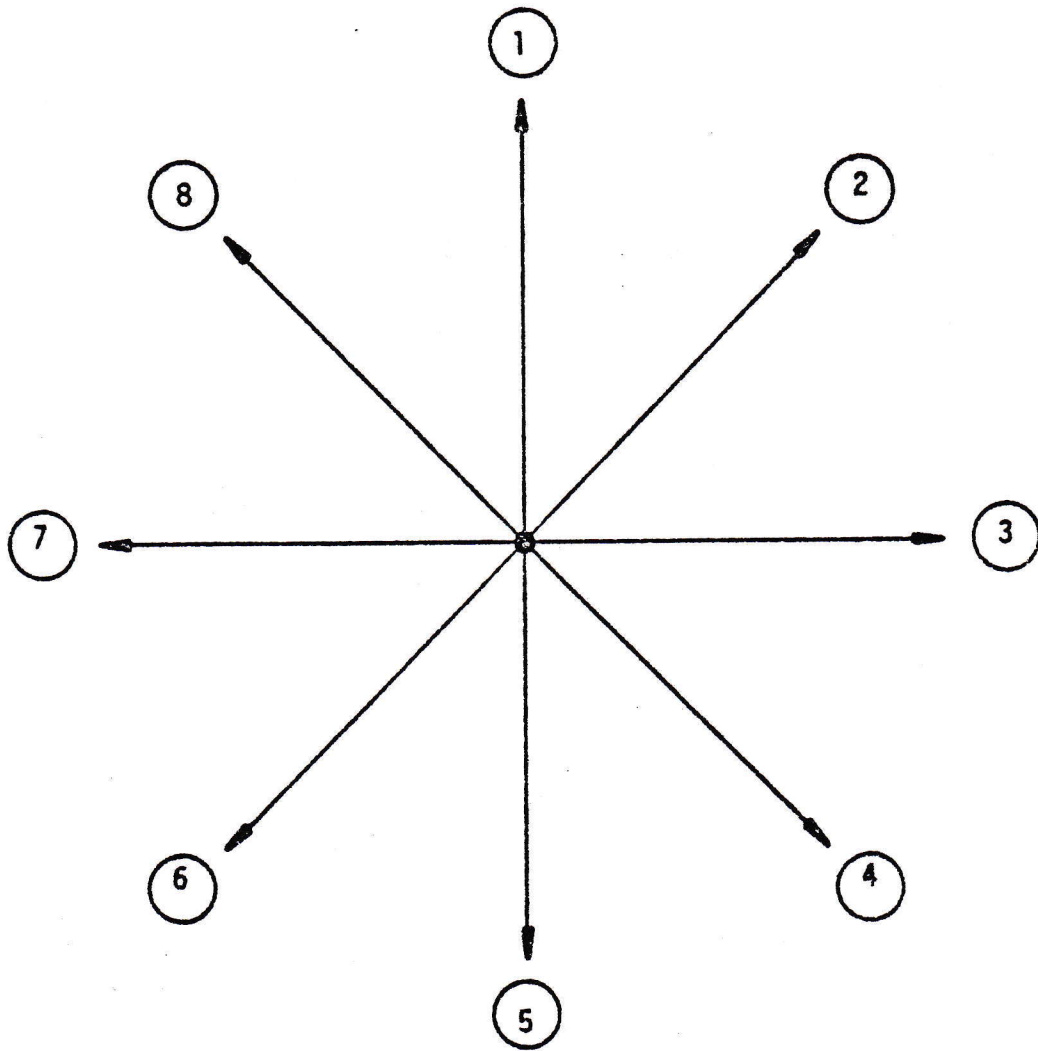


Figure 2 Direction Chart

(or target point) was assumed to be 250 nautical miles above the surface of the earth and circular. The total integration time was set to one prior orbital period, or -5631 seconds for this orbital altitude.

Graphic results of the integration are presented in Figures 3.1 to 3.8. The orbital plane (X-Y plane) is shown in these figures with the origin of the coordinate system being the target point for rendezvous. The relative position of the shuttle with respect to the target point is presented for one prior orbital period. Positions of the shuttle after 0, -2000, -4000, and -5631 seconds are shown on each trajectory along with the magnitude and direction of the velocity at the origin (time = $t = 0$). Also, stable stationkeeping points (on the X axis) are denoted.

- Shuttle Position at $t = 0$ sec
- △ Shuttle Position at $t = -2000$ sec
- ◇ Shuttle Position at $t = -4000$ sec
- Shuttle Position at $t = -5631$ sec
- ◇ Possible Stable Stationkeeping Position

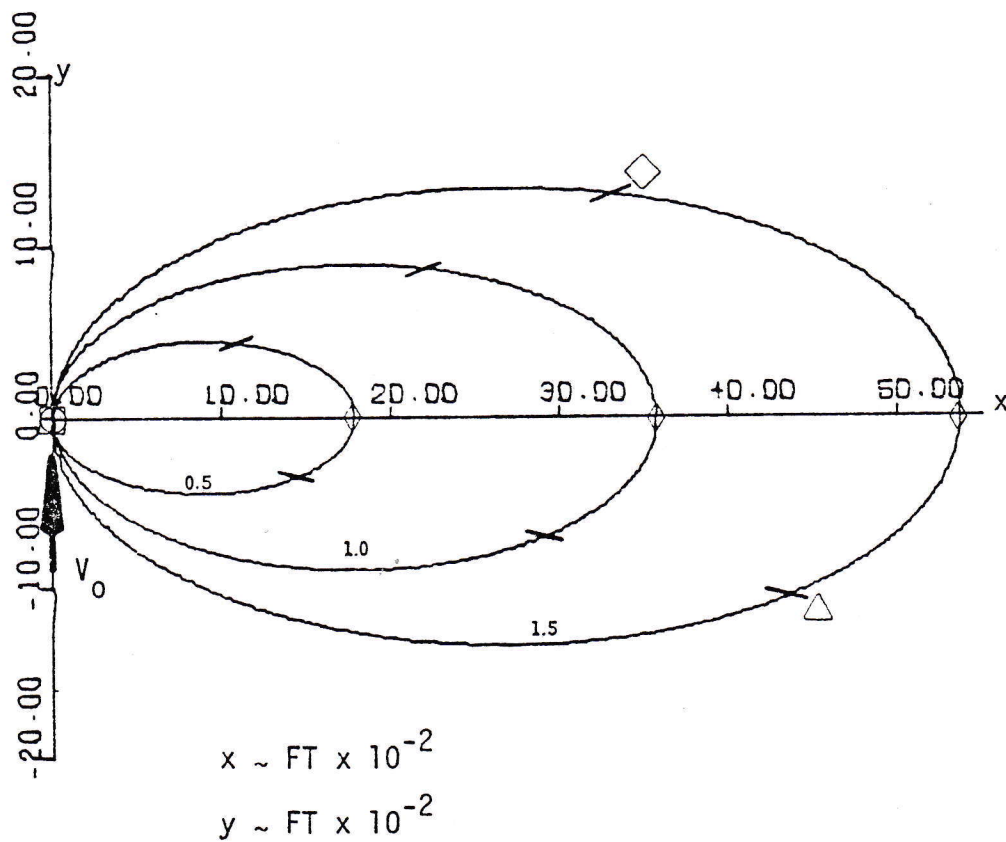


Figure 3.1 Negative Time Integration of Direction 1 Approach

- Shuttle Position at $t = 0$ sec
- △ Shuttle Position at $t = -2000$ sec
- ◇ Shuttle Position at $t = -4000$ sec
- Shuttle Position at $t = -5631$ sec
- ◇ Possible Stable Stationkeeping Position

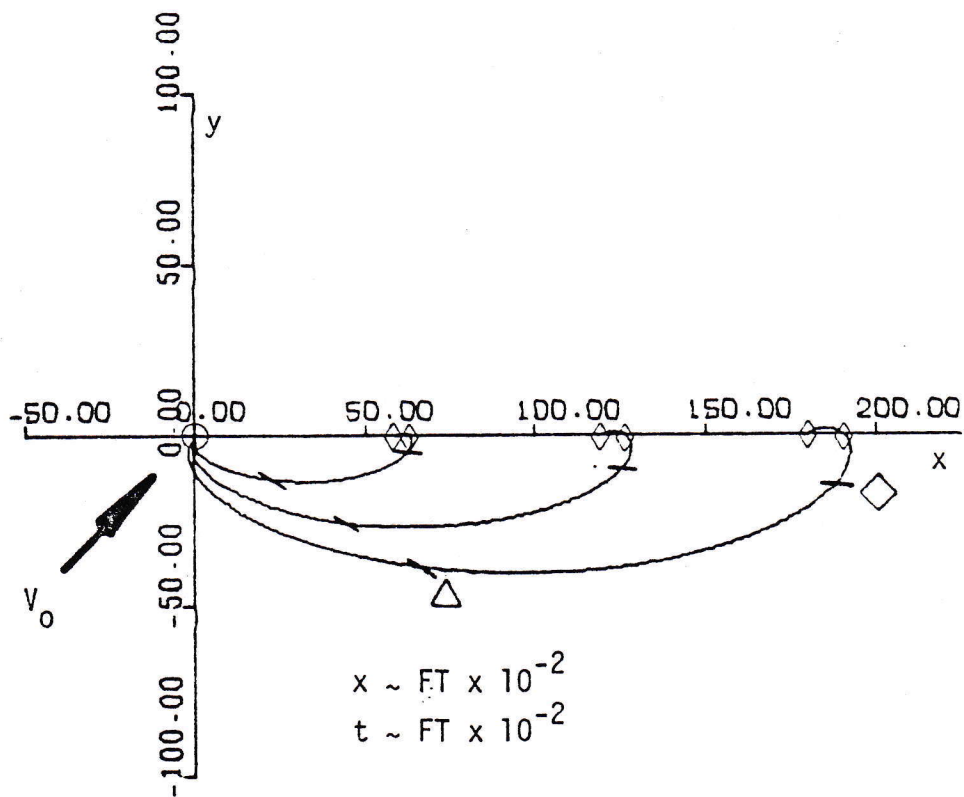


Figure 3.2 Negative Time Integration of Direction 2 Approach

- Shuttle Position at t = 0 sec
- △ Shuttle Position at t = -2000 sec
- ◇ Shuttle Position at t = -4000 sec
- Shuttle Position at t = -5631 sec

- ◇ Possible Stable Stationkeeping Position

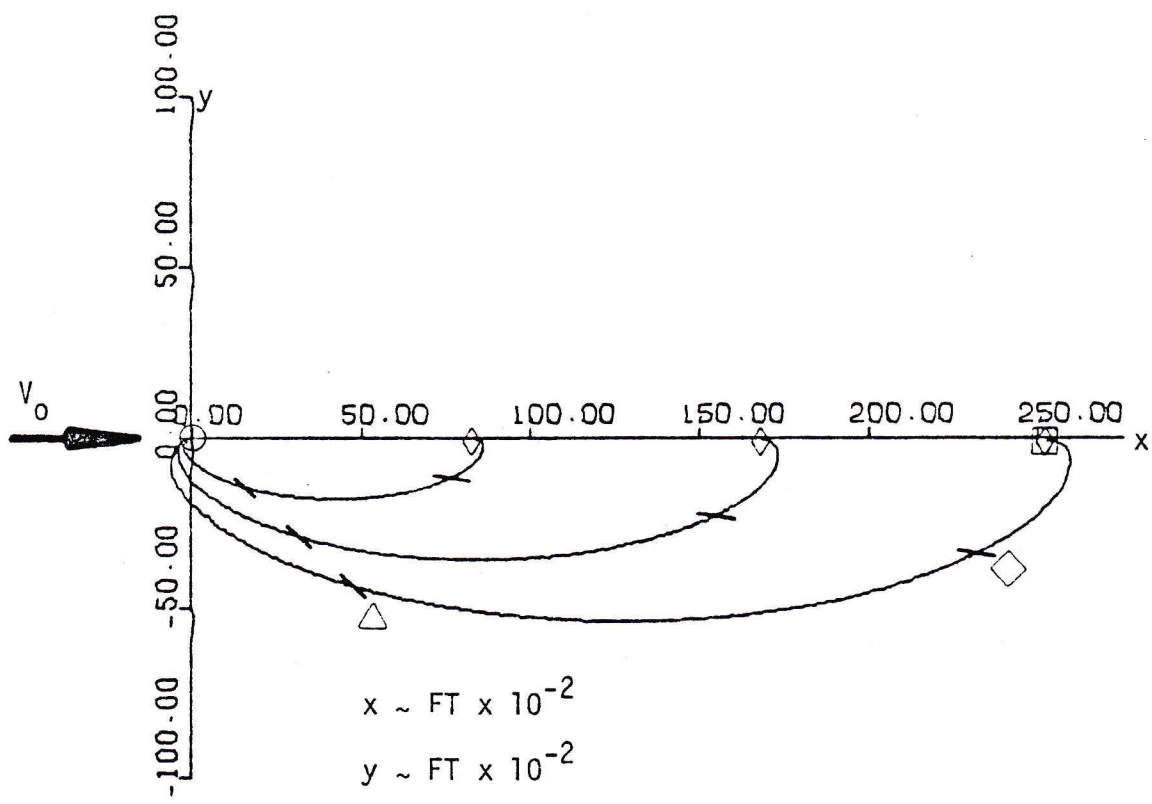


Figure 3.3 Negative Time Integration of Direction 3 Approach

- Shuttle Position at $t = 0$ sec
- △ Shuttle Position at $t = -2000$ sec
- ◇ Shuttle Position at $t = -4000$ sec
- Shuttle Position at $t = -5631$ sec
- ◇ Possible Stable Stationkeeping Position

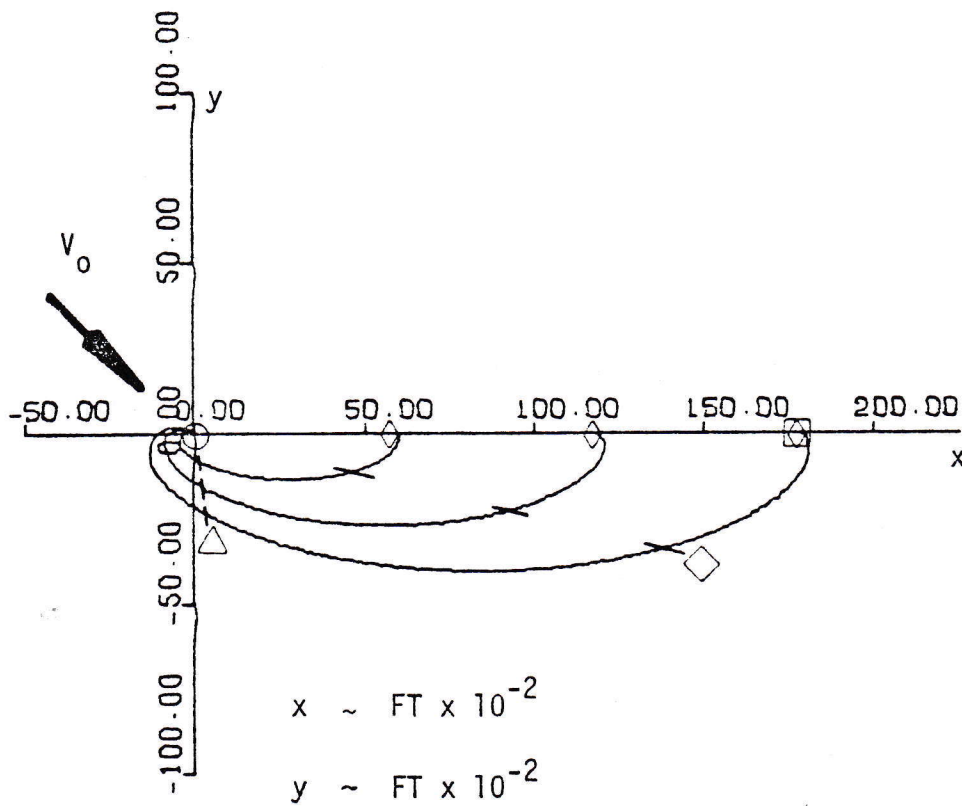


Figure 3.4 Negative Time Integration of Direction 4 Approach

- Shuttle Position at $t = 0$ sec
- △ Shuttle Position at $t = -2000$ sec
- ◇ Shuttle Position at $t = -4000$ sec
- Shuttle Position at $t = -5631$ sec
- ◇ Possible Stable Stationkeeping Position

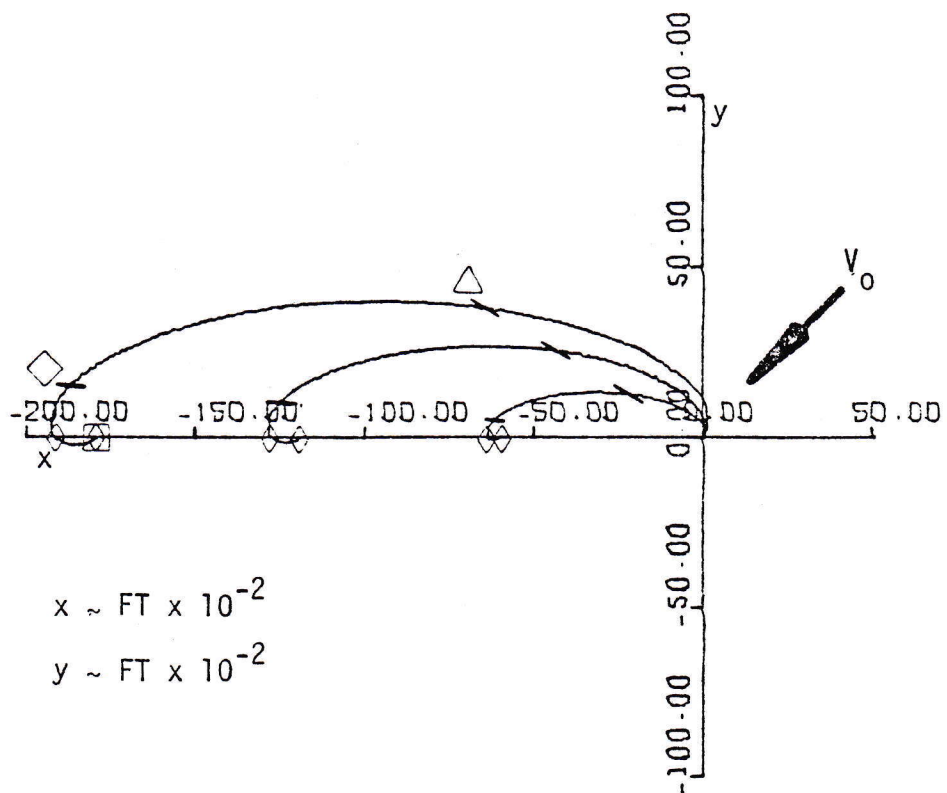


Figure 3.6 Negative Time Integration of Direction 6 Approach

- Shuttle Position at $t = 0$ sec
- △ Shuttle Position at $t = -2000$ sec
- ◇ Shuttle Position at $t = -4000$ sec
- Shuttle Position at $t = -5631$ sec

- ◇ Possible Stable Stationkeeping Position

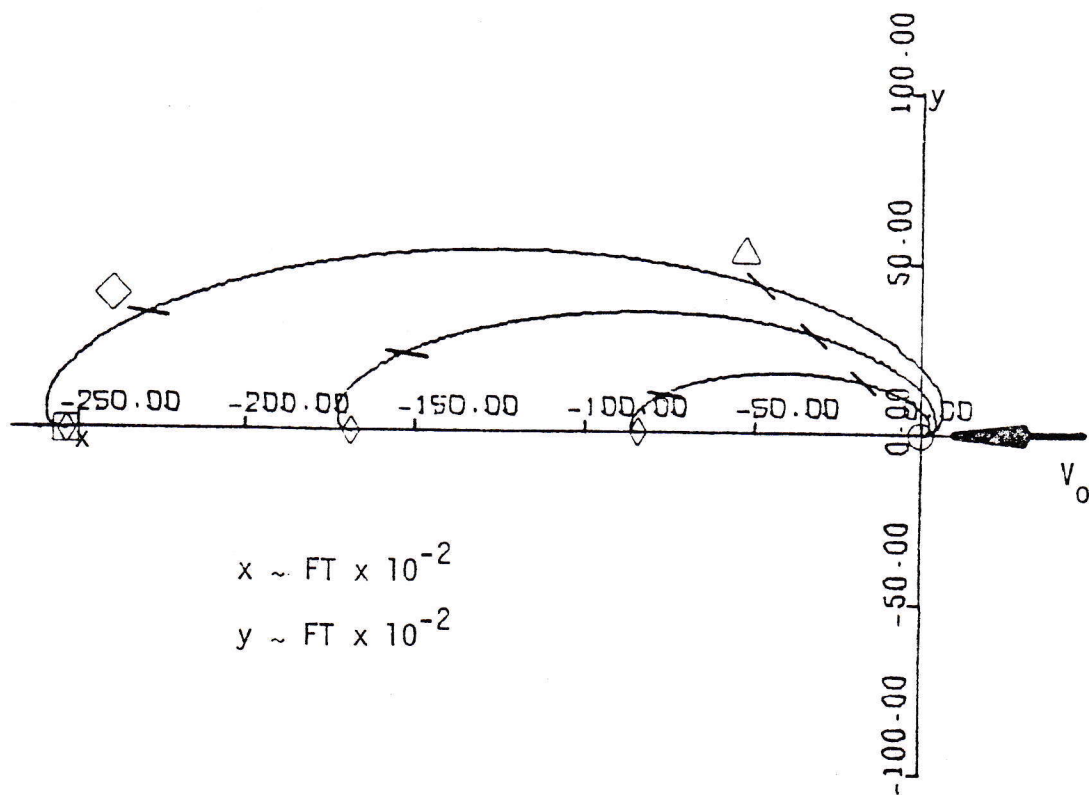


Figure 3.7 Negative Time Integration of Direction 7 Approach

- Shuttle Position at $t = 0$ sec
- △ Shuttle Position at $t = -2000$ sec
- ◇ Shuttle Position at $t = -4000$ sec
- Shuttle Position at $t = -5631$ sec
- ◇ Possible Stable Stationkeeping Position

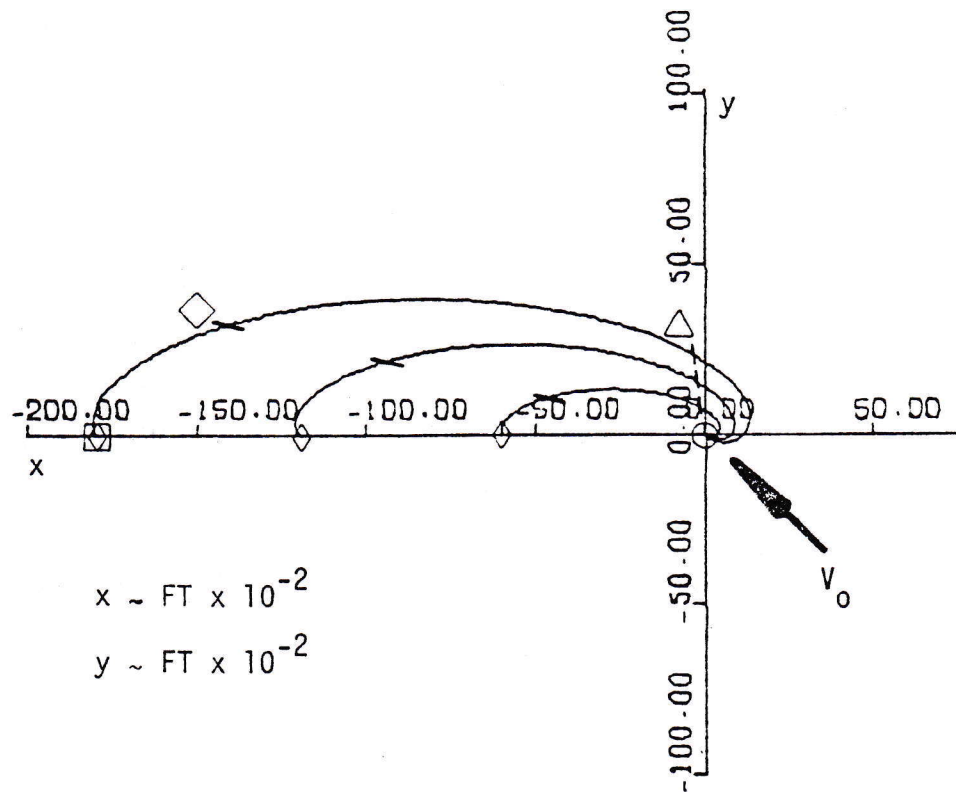


Figure 3.8 Negative Time Integration of Direction 8 Approach

Figure 3.1

Figure 3.1 shows trajectories for a shuttle with initial velocities at the origin in direction 1 (see figure 2). The three trajectories shown were generated by varying the magnitude of the velocity at the origin ($\vec{V}_0 = 0.5$ fps, 1.0 fps, and 1.5 fps). The relative motion shown is unique in that it is periodic with a period of 5631 seconds. This is identical to the period of the target body (origin) around the earth. It can be seen that an initial ($t = 0$) velocity magnitude of 1.0 fps (in direction 1) will result in a X axis crossing after -2815 seconds (at $X = 3650$ ft, $Y = 0$ ft). Thus, in actual practice, this position would be selected as the stable stationkeeping point from which to initiate a rendezvous. The velocity necessary to effect a rendezvous would be identical to the velocity computed by the negative time integration procedure for this position ($X = 3650$ ft, $Y = 0$ ft, $t = -2815$ sec.). The RCS and VRCS thrusters must be used to establish this velocity at the stationkeeping point. This comprises the first impulse. After coasting for 2815 seconds, the shuttle would arrive at the target body (origin) with a relative velocity of 1.0 fps. The shuttle will approach the origin from below, i.e., a direction 1 approach. Since the final relative velocity at the origin is greater than 0.2 fps, the payload cannot be captured by the RMS due to the structural constraints imposed. Therefore, the velocity must be reduced to 0.2 fps (or less) by once more firing the RCS or VRCS thrusters. This would comprise the second impulse of the trajectory, hence the notation two impulse trajectory. It must be noted that in practice, the rendezvous would actually be targeted for an offset location about 50 ft from the

target body. Of primary significance in Figure 3.1 is the fact that the stable stationkeeping distance is proportional to the relative velocity at encounter. Thus, a similar trajectory does exist and may be determined for any desired stationkeeping distance on the X axis. Such a trajectory offers many advantages. The moderate coast time (time between first and second impulses) could be used to perform systems checks while the shuttle is enroute. The initial and final velocities have Y components only ($\dot{X} = 0$). The first impulse velocity is easily initiated and the final approach velocity is easily negated from a nose-down shuttle attitude with little danger of plume impingement. On final approach, the tail of the shuttle would be allowed to go above the target body before the RCS or VRCS thrusters are fired (see Figure 4). Such a constant nose down shuttle attitude will allow excellent crew visibility during the entire rendezvous. This attitude will also result in a final approach which will appear (to the shuttle crew) to bring the target body down, over the tail and above the cargo bay area of the shuttle. This is identical to the optimal approach scenario as described earlier. The trajectory is very interesting since it is periodic. If necessary (RMS malfunction, satellite tumbling, etc.) the shuttle would return to the initial stationkeeping point with no further thrust required. Also, the trajectory is easily altered while enroute to improve the accuracy of final approach. In addition, the total ΔV consumed by this periodic trajectory is relatively low, and since total ΔV is a direct measurement of the fuel consumed, this is an important consideration.

Shuttle not to Scale

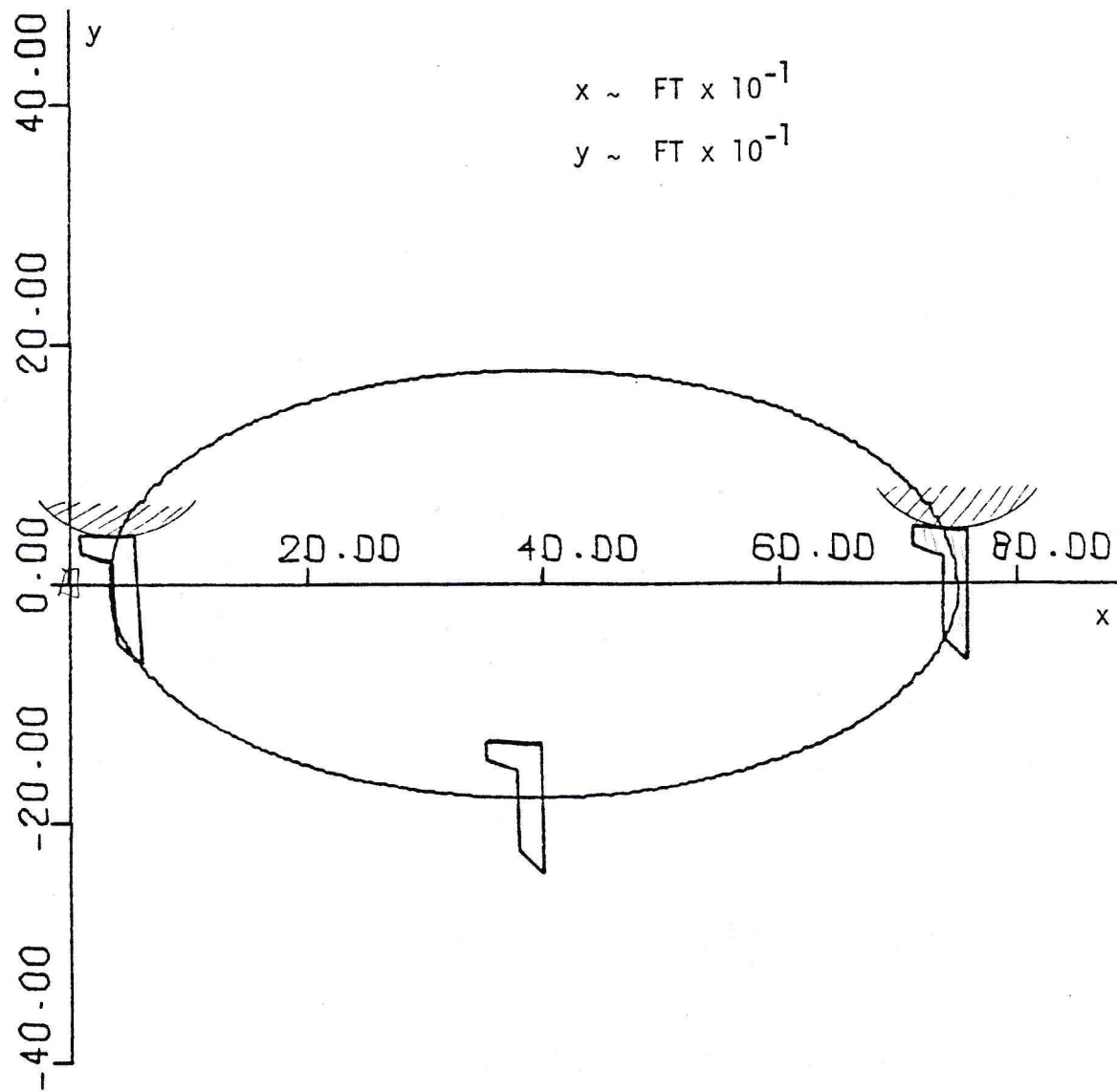


Figure 4 Constant Shuttle Attitude Without Plume Impingement

Figures 3.2, 3.3, 3.4

The trajectories in Figure 3.2 were determined from an initial velocity in direction 2 (see Figure 2). Once again, three velocity magnitudes ($\vec{V}_0 = 0.5$ fps, 1.0 fps, and 1.5 fps) are presented. The shuttle position at various times during the trajectories have been specified. It can be seen that two stable stationkeeping points (on X axis) exist for each trajectory. For $\vec{V}_0 = 1.0$ fps, these locations are $X = 2390$ ft and $X = 2541$ ft. The coast times for rendezvous from these locations are 5631 sec and 5808 sec respectively. Once again, a linear relationship between stationkeeping distance and \vec{V}_0 may be seen. The trajectories are not periodic and crew visibility and plume impingement constraints are not easily met with a constant shuttle attitude.

The rendezvous trajectories shown in Figure 3.3 are similar with those discussed above with the exception of the direction of final approach to the target point (origin). Direction 3 approaches are presented in this case. Once more, the linear relationship between stationkeeping distance and \vec{V}_0 is noticed. Also, the trajectories are not periodic. Crew visibility would not be possible at all times with a constant shuttle attitude since the trajectory takes the shuttle from behind the target point, to below and then in front of the target.

Figure 3.4 shows rendezvous trajectories with \vec{V}_0 values in direction 4. The results are similar to those described above and the same comments apply. Again, shuttle position at various times during the trajectories have been noted.

Operational techniques may be employed in these latter (Figures 3.2, 3.3, 3.4) trajectories to minimize plume effects and to allow for

adequate crew visibility. One possible method to avoid plume impingement would be to target for a point within 50 ft of the origin such that the shuttle would arrive with a relative velocity which is perpendicular to a radius vector to the origin at that point. Then, once the plane of the RCS thrusters has passed the payload, the thrusters could be fired (second impulse) without any possibility of plume impingement. Such a case is described in Figure 5.

Crew visibility constraints are more difficult to meet since several of the trajectories circle about the target point in such a manner that a constant shuttle attitude will not enable the mission specialist to view the target at all times during the final rendezvous. In these cases, it may be necessary to give the shuttle an angular velocity which will rotate it at the proper rate to enable vision of the target point. Such a case is presented in Figure 6. This angular velocity would then be cancelled upon arrival at the target point. However, to cancel the angular velocity it would be necessary to create an opposite moment about the shuttle center of mass in order that the motion may be completely stopped (no linear component left). This would expell propellant particles in two opposite directions from the shuttle. Due to the expansion of this plume (to 90°), impingement could not be avoided. Thus, for rendezvous to low density or sensitive payloads, trajectories such as this (non-constant shuttle attitude) do not appear feasible.

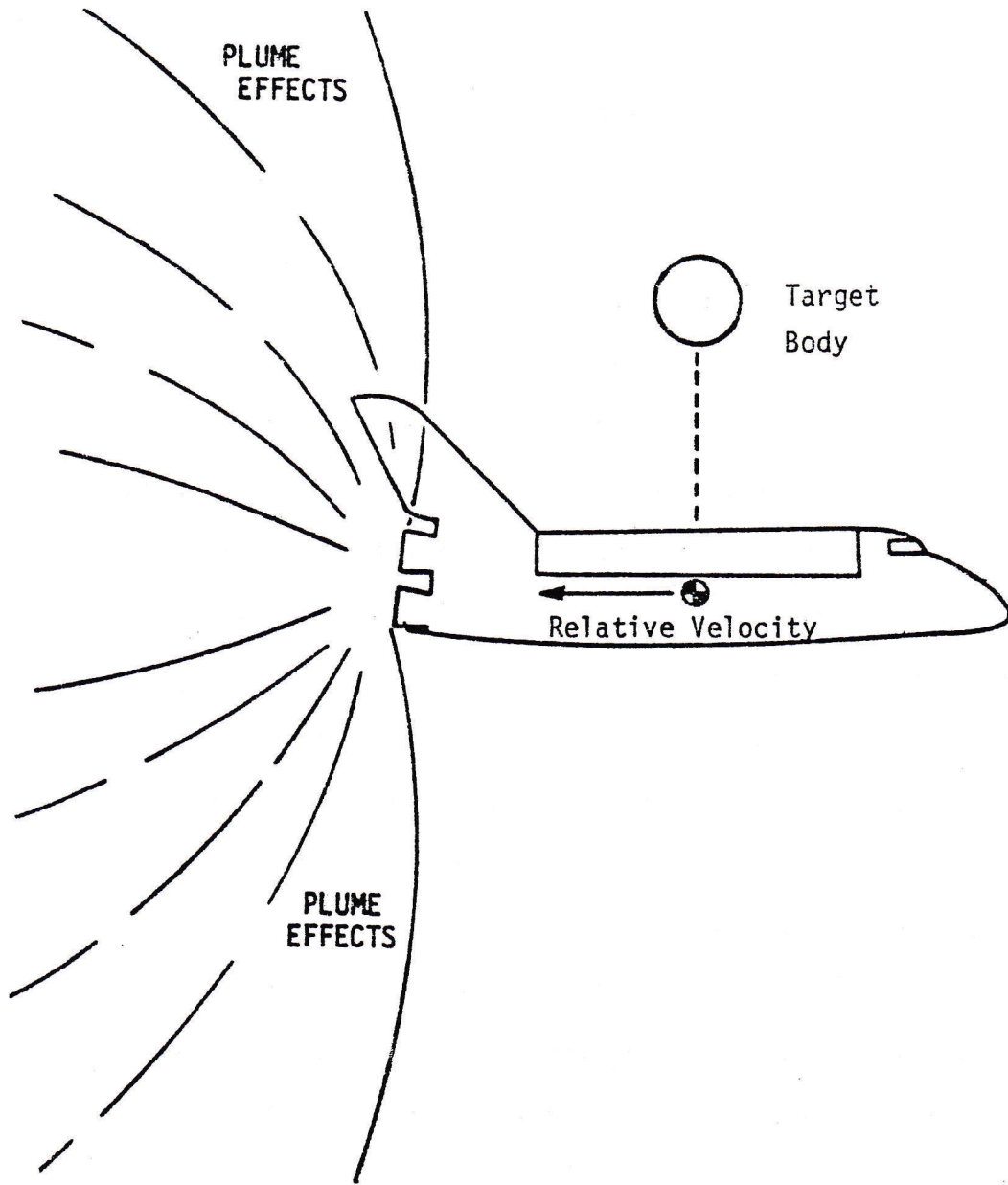


Figure 5 Shuttle Fly-By to Eliminate Plume Impingement

Shuttle not to Scale

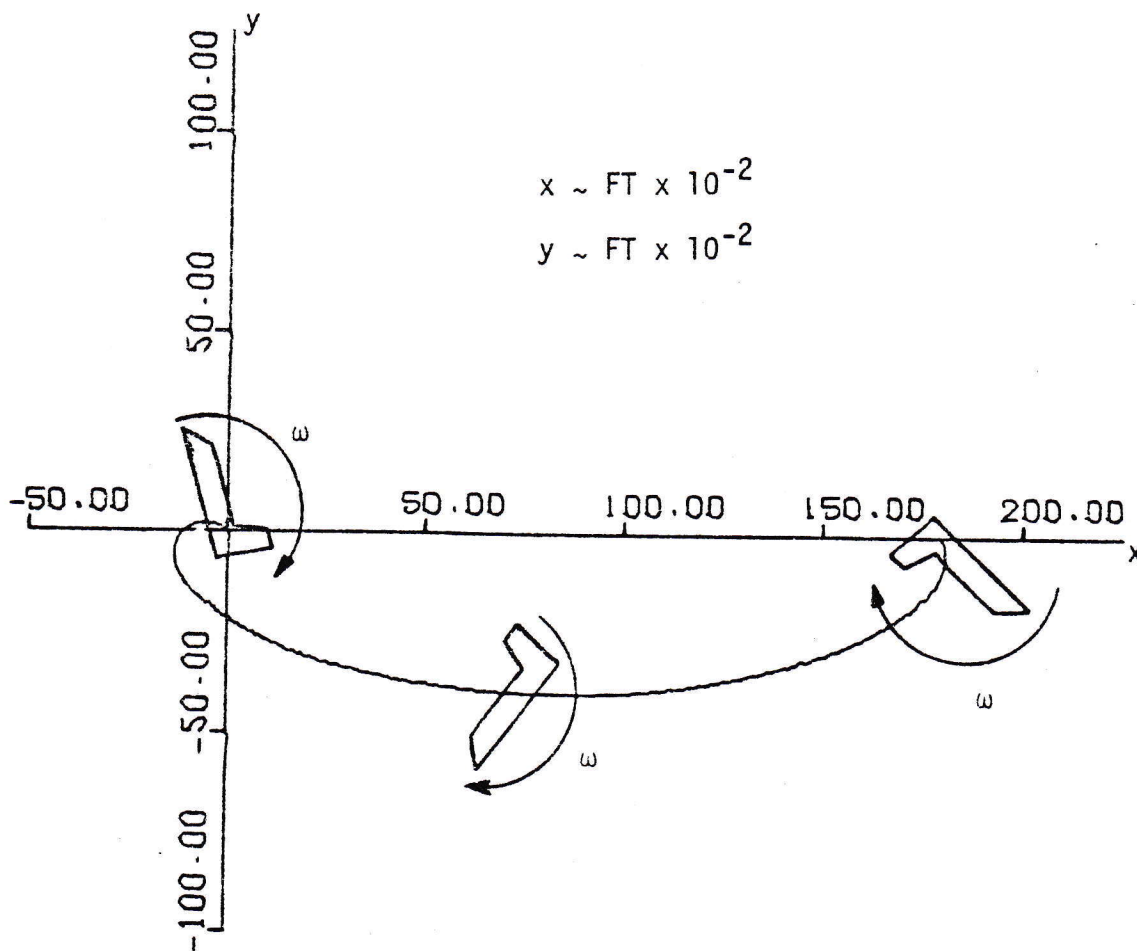


Figure 6 Rotational Procedure to Maintain Visibility

Figures 3.5, 3.6, 3.7, 3.8

By inspection, it may be seen that the trajectories shown in these figures are mirror images of those shown in Figures 3.1 to 3.4 and the same comments apply. Since the results of one initial velocity direction may be applied (by taking the negative) to the opposite direction, only directions 1 through 4 will be analyzed in the remainder of this text to avoid an unnecessary duplication in effort.

CHAPTER 4

One Impulse Rendezvous Trajectories

Due to plume impingement considerations, it would be very desirable if rendezvous trajectories could be identified which had final approach velocities of less than or equal to 0.2 fps. This would eliminate the need for a second impulse to slow the shuttle to allow RMS capture and therefore would eliminate any possibility of plume impingement. Such a maneuver is called a one impulse trajectory since the one thrust necessary for rendezvous would be applied at the station-keeping point. The procedure to determine these one impulse trajectories is essentially the same as the procedure described in the previous chapter for the two impulse trajectories. The only difference between the one and two impulse analysis is the magnitude of the velocity at the origin (\vec{V}_0) which is used in the negative time integration procedure to determine the previous path of the shuttle. Since one impulse trajectories are constrained to have a final maximum closure rate of 0.2 fps, this is also the maximum \vec{V}_0 magnitude which may be used.

For simulation purposes, the orbit of the origin (target point) was assumed to be 250 nm above the surface of the earth and circular. The total integration time was set to one prior orbital period, or -5631 sec. Figures 7.1 to 7.4 represent results of the negative time integration. Three velocity magnitudes (0.1 fps, 0.15 fps, and 0.2 fps) in each of four directions (1 through 4) are presented for the one impulse case.

- Shuttle Position at $t = 0$ sec
- △ Shuttle Position at $t = -2000$ sec
- ◇ Shuttle Position at $t = -4000$ sec
- Shuttle Position at $t = -5631$ sec
- ◇ Possible Stable Stationkeeping Position

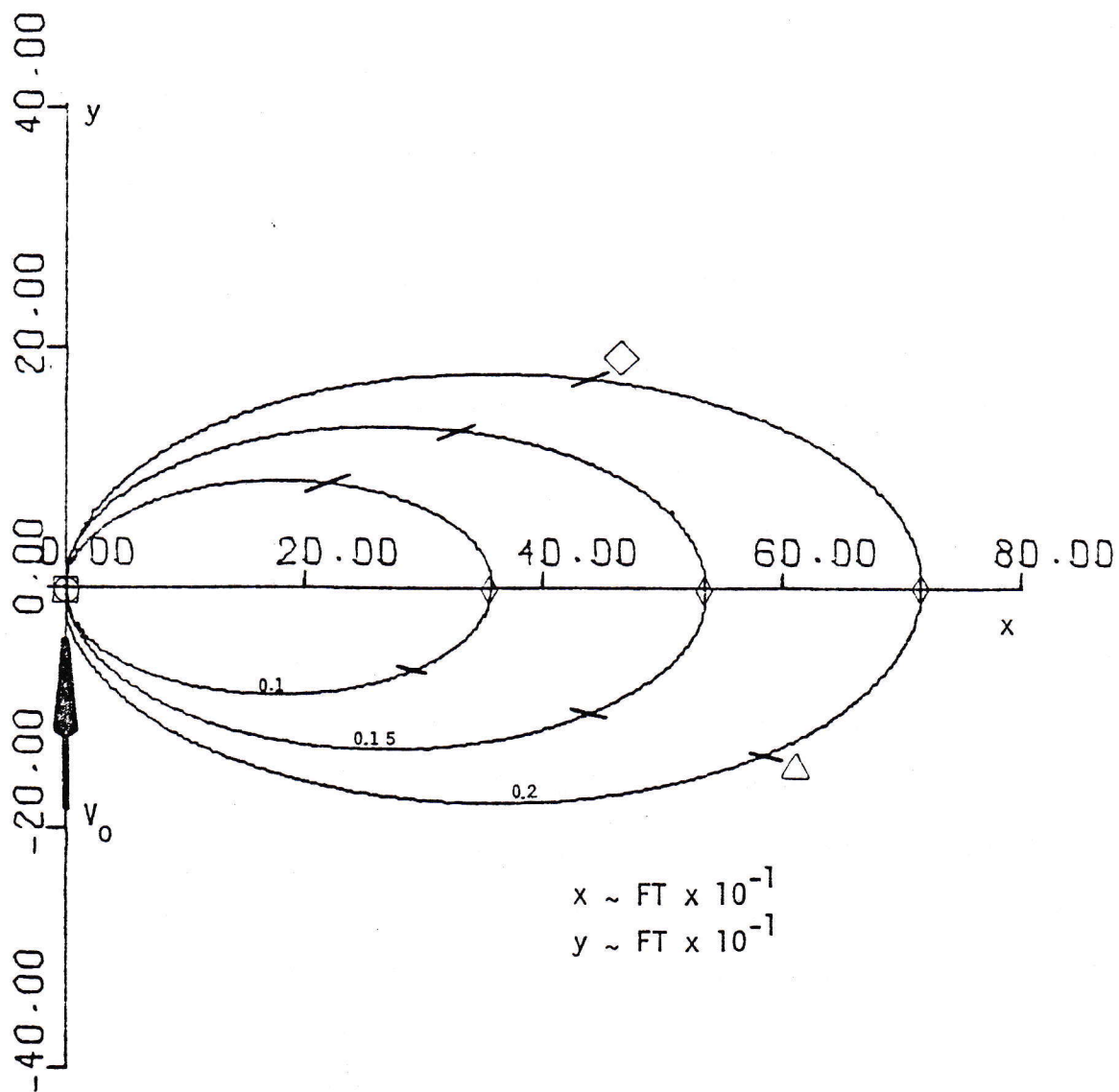


Figure 7.1 Negative Time Integration of Direction 1 Approach

- Shuttle Position at $t = 0$ sec
- △ Shuttle Position at $t = -2000$ sec
- ◇ Shuttle Position at $t = -4000$ sec
- Shuttle Position at $t = -5631$ sec
- ◇ Possible Stable Stationkeeping Position

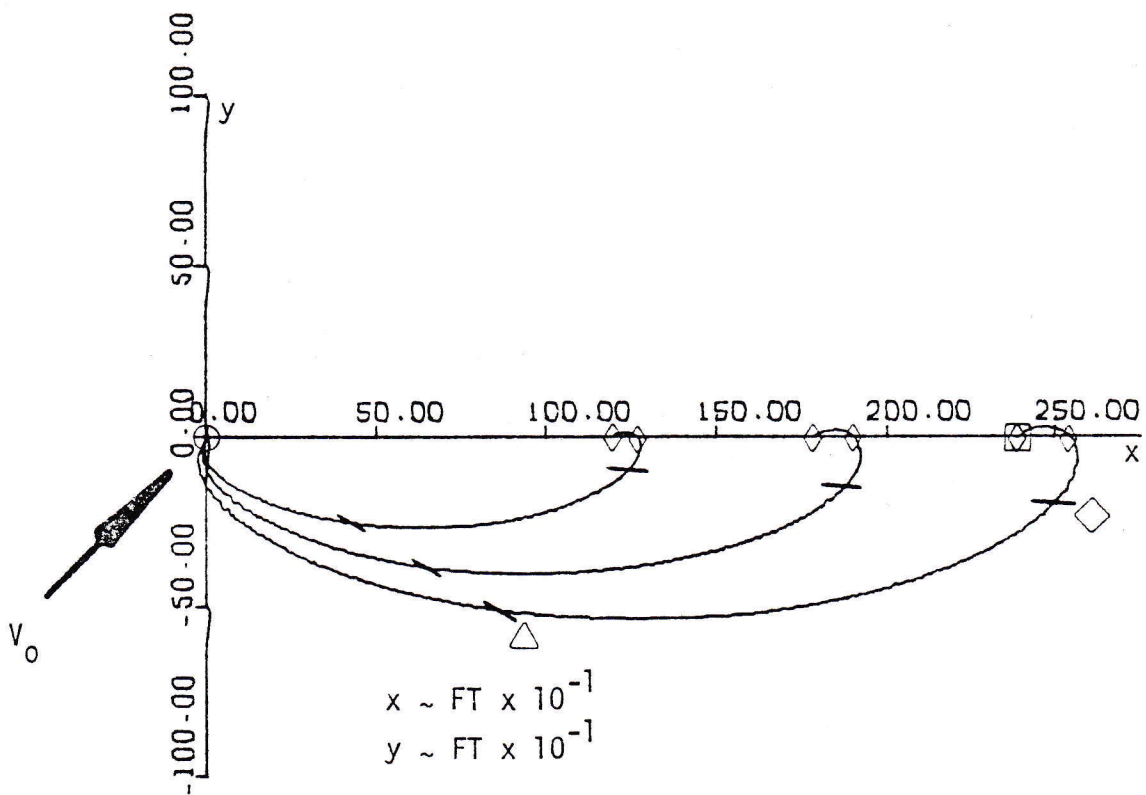


Figure 7.2 Negative Time Integration of Direction 2 Approach

- Shuttle Position at $t = 0$ sec
- △ Shuttle Position at $t = -2000$ sec
- ◇ Shuttle Position at $t = -4000$ sec
- Shuttle Position at $t = -5631$ sec
- ◇ Possible Stable Stationkeeping Position

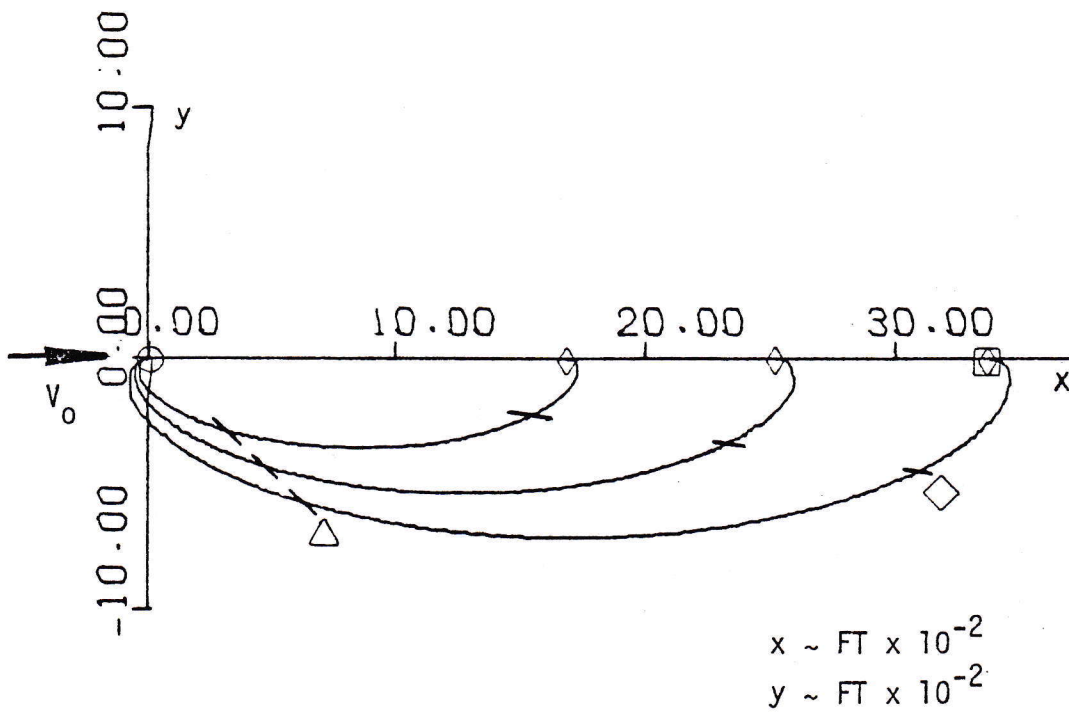


Figure 7.3 Negative Time Integration of Direction 3 Approach

- Shuttle Position at $t = 0$ sec
- △ Shuttle Position at $t = -2000$ sec
- ◇ Shuttle Position at $t = -4000$ sec
- Shuttle Position at $t = -5631$ sec
- ◇ Possible Stable Stationkeeping Position

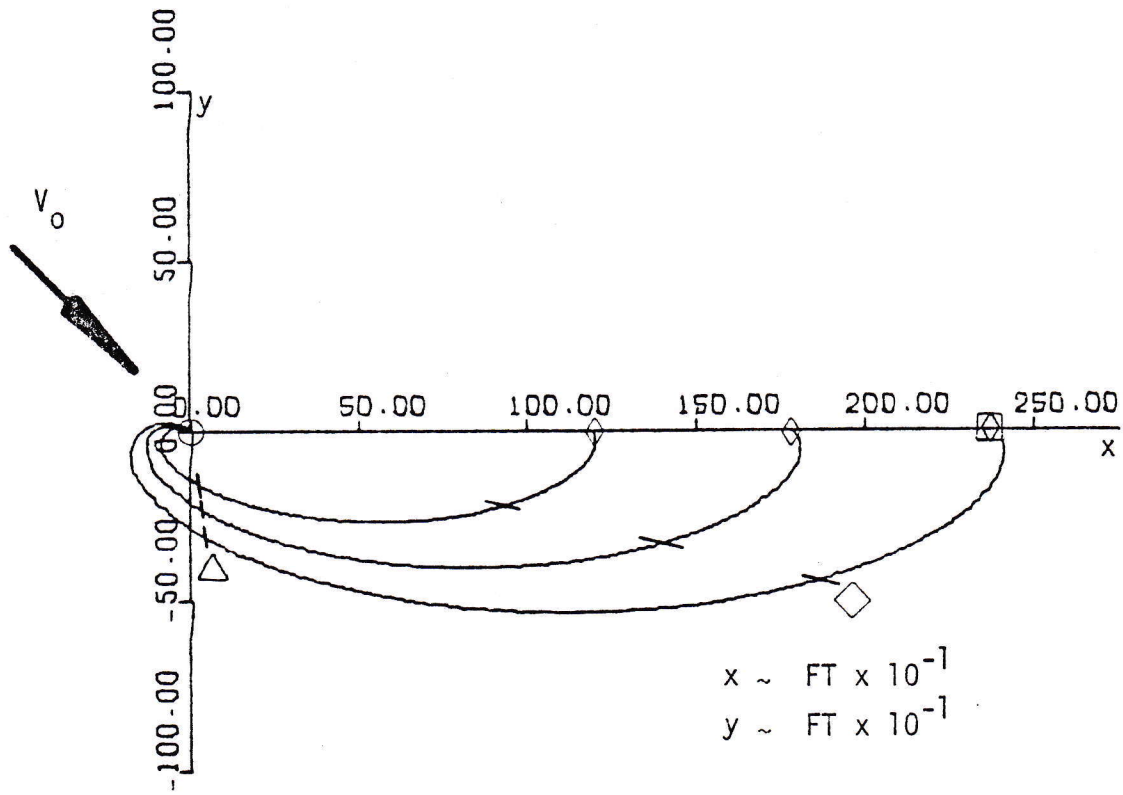


Figure 7.4 Negative Time Integration of Direction 4 Approach

Figures 7.1 to 7.4

It may be seen that the trajectories denoted by Figures 7.1 to 7.4 are directly related to those of Figures 3.1 to 3.4, the only difference being a scale factor determined by a ratio of the \vec{V}_0 values of each individual trajectory. Accordingly, the same comments apply. Due to RMS constraints, the $\vec{V}_0 = 0.2$ fps trajectories shown in Figures 7.1 to 7.4 form a one impulse rendezvous envelope for the various approach directions. For example, a periodic (direction 1, Figure 7.1) rendezvous with $\vec{V}_0 = 0.2$ fps results in a X axis stationkeeping location of 717 feet. A larger \vec{V}_0 value results in a proportionally larger stationkeeping distance. Thus, the maximum limit on stationkeeping distance for a one-impulse, periodic rendezvous is 717 feet.

CHAPTER 5

Generalized Rendezvous Techniques

The negative time integration procedure described in the preceding chapters is a very accurate means of determining rendezvous trajectories for specific approach conditions. However, as pointed out previously, it is not useful in determining a rendezvous trajectory when only the initial shuttle location relative to the target point is known. This chapter will discuss the latter problem and present a generalized rendezvous technique.

R. S. Dunning³ has used an approach different from that presented in Chapter 2 to formulate another set of differential equations for two body motion. He then linearized the equations to arrive at the form shown as Equations (21). They are known as the Clohessey-Wiltshire Equations.

$$\begin{aligned}\dot{\xi} &= \omega_{AVG} r_0 \cos\alpha \frac{\tan\alpha[12\pi P - 14 \tan(\pi P)] - 1}{8 \tan(\pi P) - 6\pi P} \\ \dot{\eta} &= \omega_{AVG} r_0 \cos\alpha \frac{\tan\alpha[6\pi P \cot(2\pi P) - 4] + 2 \tan(\pi P)}{8 \tan(\pi P) - 6\pi P}\end{aligned}\quad (21)$$

These equations give the velocity components $(\dot{\xi}, \dot{\eta})$ which are necessary to effect a rendezvous with the origin of the ξ, η coordinate system from an original position (ξ_0, η_0) in that system. As applied to proximity operations, the variable, r_0 , is the initial distance between the shuttle and target. Also, $\alpha = \arctan\left(\frac{\eta_0}{\xi_0}\right)$ where ξ_0 and η_0 are the shuttle stationkeeping locations in a coordinate system centered at the target

point with η directed radially outward from the earth. ξ and η are perpendicular, lie in the orbital plane, and the positive ξ axis extends in the direction defined by $\vec{\omega}_{AVG} \times \vec{\eta}$ where $\vec{\omega}_{AVG}$ is the average angular velocity of $\vec{\eta}$ with magnitude ω_{AVG} (see Figure 8). $\dot{\xi}_0$ and $\dot{\eta}_0$ are the necessary rates of change of ξ and η to affect a rendezvous from the original shuttle location, ξ_0 and η_0 . The rendezvous time, t_r , or amount of time spent coasting between the first impulse and final approach, is represented as a functional portion of one orbital period, T_p . This ratio is denoted by the parameter P . Also, the rendezvous time, t_r , is dependent on the initial shuttle position and the desired average closure rate, \dot{r}_{AVG} .

$$\omega_{AVG} = \frac{2\pi}{T_p}, \quad t_r = \frac{R_0}{\dot{r}_{AVG}}, \quad P = \frac{t_r}{T_p}, \quad T_p = \frac{2a^{3/2}\pi}{\sqrt{GM}} \quad (22)$$

By introducing this last equation, where a is the semi-major axis of the orbit and GM is the gravitational parameter of the earth, and by using trigonometric relationships for $\sin\alpha$, $\cos\alpha$, and $\tan\alpha$, Dunning's equations may be further simplified.

$$\dot{\xi} = \frac{\omega_{AVG} [12\eta\lambda - 14\eta \tan(\lambda) - \xi]}{8 \tan(\lambda) - 6\lambda} \quad (23)$$

$$\dot{\eta} = \frac{\omega_{AVG} [6\eta\lambda \cot(2\lambda) - 4\eta + 2\tan(\lambda)]}{8 \tan(\lambda) - 6\lambda}$$

where $\lambda = \frac{R_0 \omega_{AVG}}{2 \dot{r}_{AVG}} \quad (24)$

The coordinates used by Dunning differ from those used earlier in the Lagrangian analysis (Chapter 2) only by a 180° rotation about the Y

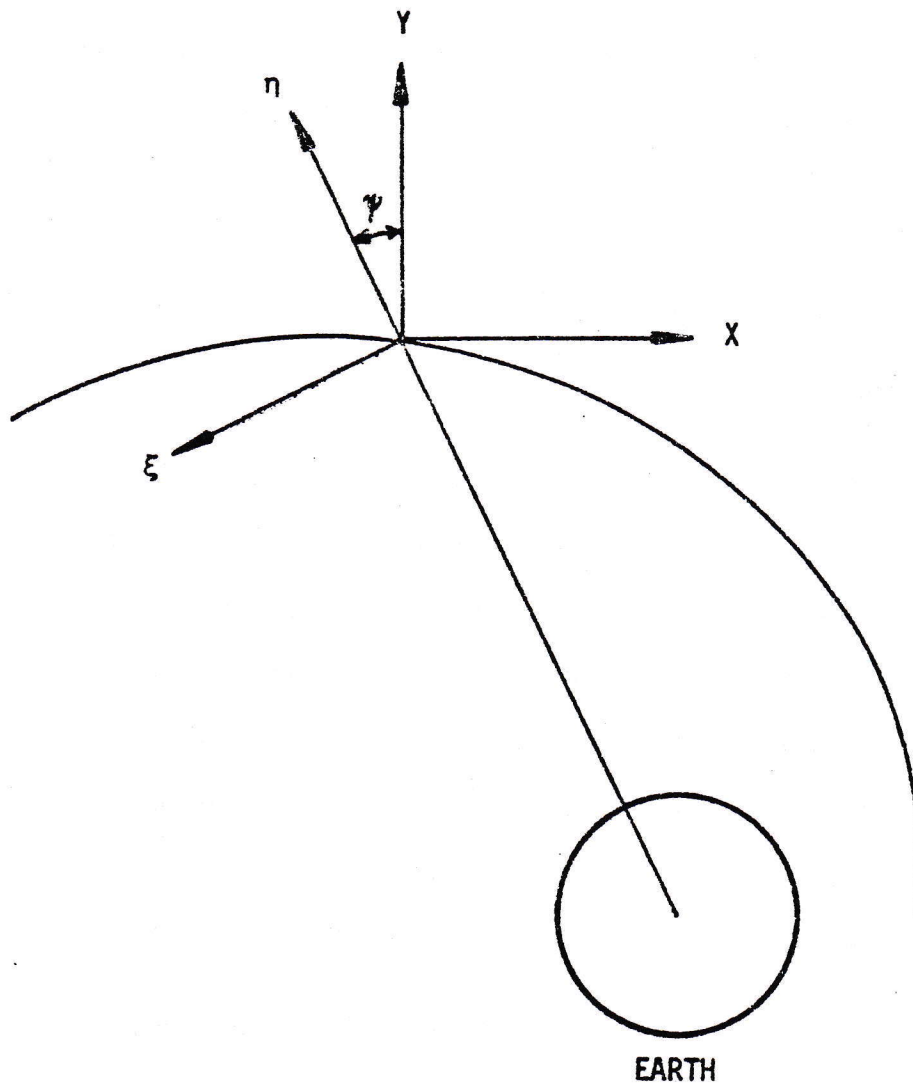


Figure 8 ξ - η Coordinates vs. X-Y Coordinates

axis and a rotation of ψ about the Z axis. For the case of a circular orbit (which has been assumed), $\psi = 0$ and a coordinate rotation would further simplify equations (23). For $\psi = 0$, ξ and η would simply be replaced by $-X$ and Y respectively. Equations (25) represent this simplified form which has been rotated to the target centered (X, Y, Z) coordinate system as defined previously.

$$\begin{aligned}\dot{X} &= \frac{\omega_{AVG} [14Y \tan(\lambda) - 12Y\lambda - X]}{8 \tan(\lambda) - 6\lambda} \\ \dot{Y} &= \frac{\omega_{AVG} [6Y\lambda \cot(2\lambda) - 4Y - 2X \tan(\lambda)]}{8 \tan(\lambda) - 6\lambda}\end{aligned}\tag{25}$$

Equations (25) provide a means of determining the initial velocities required of the shuttle in order to rendezvous with the target at a specified average closure rate. Data from these equations lends itself nicely to a contour plotting representation as presented in Figure 9.1, the \dot{X} component, and figure 9.2, the \dot{Y} component. This contour plotting notation was first used by D. Higgins⁴ in a similar context. The closure rate used in Figure 9 was 1.0 unit/sec. The fact that λ is nondimensional (Equation 24) leads to a nondimensional contour plot.

also, since λ contains a $\frac{R_0}{\dot{r}_{AVG}}$ term, this indicates that at a given orbital altitude, all contour plots for various average closure rates will be identical with only a scaling change. This property becomes obvious when viewing Figure 10.1, the \dot{X} component and Figure 10.2, the \dot{Y} component, which were calculated for an average closure rate of 0.2 unit/sec. Thus, a procedure becomes apparent for altering the contour

250 nm Circular Orbit

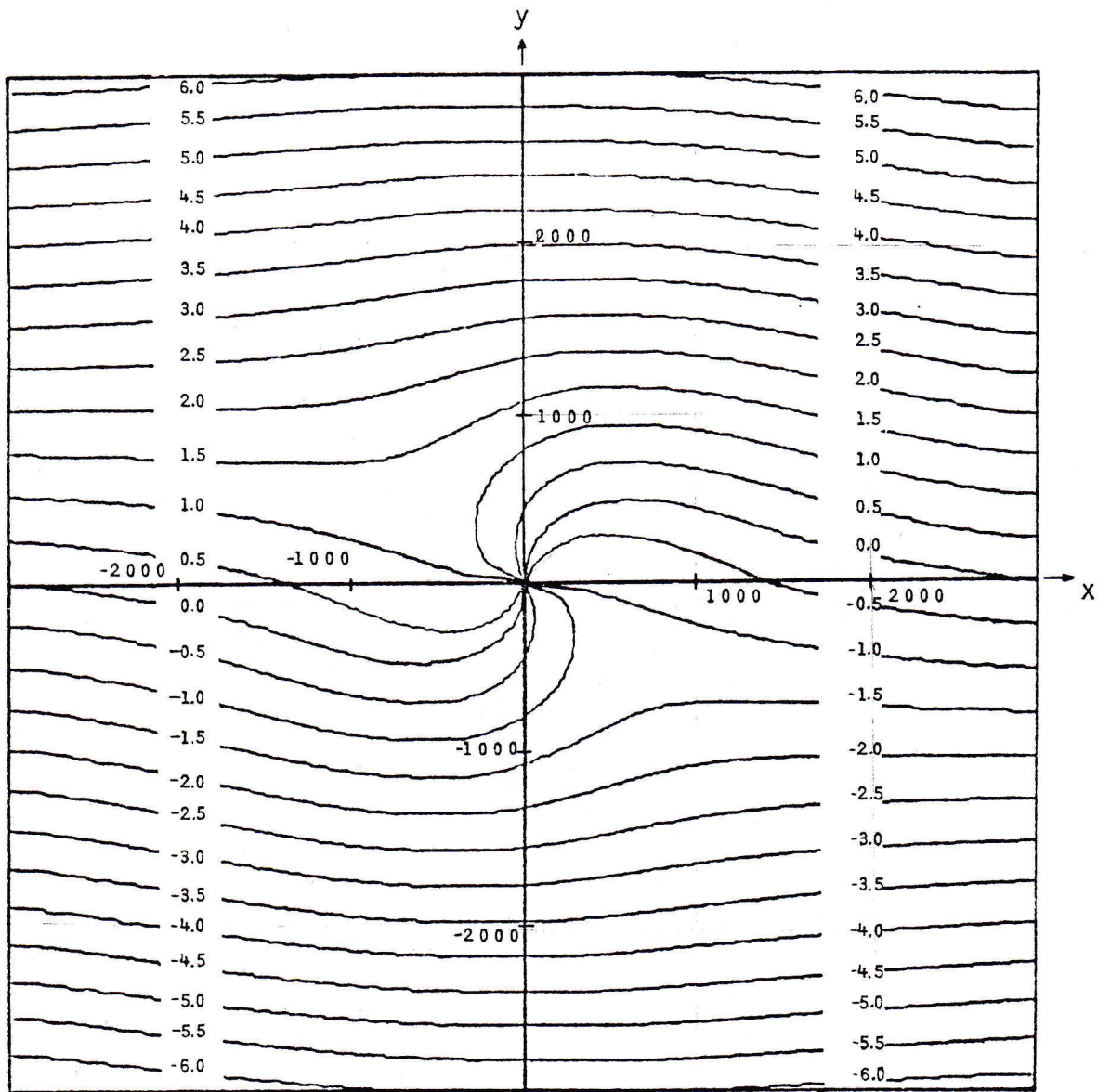


Figure 9.1 \dot{X} Rendezvous Contours at $\dot{r}_{avg} = 1.0$

250 nm Circular Orbit

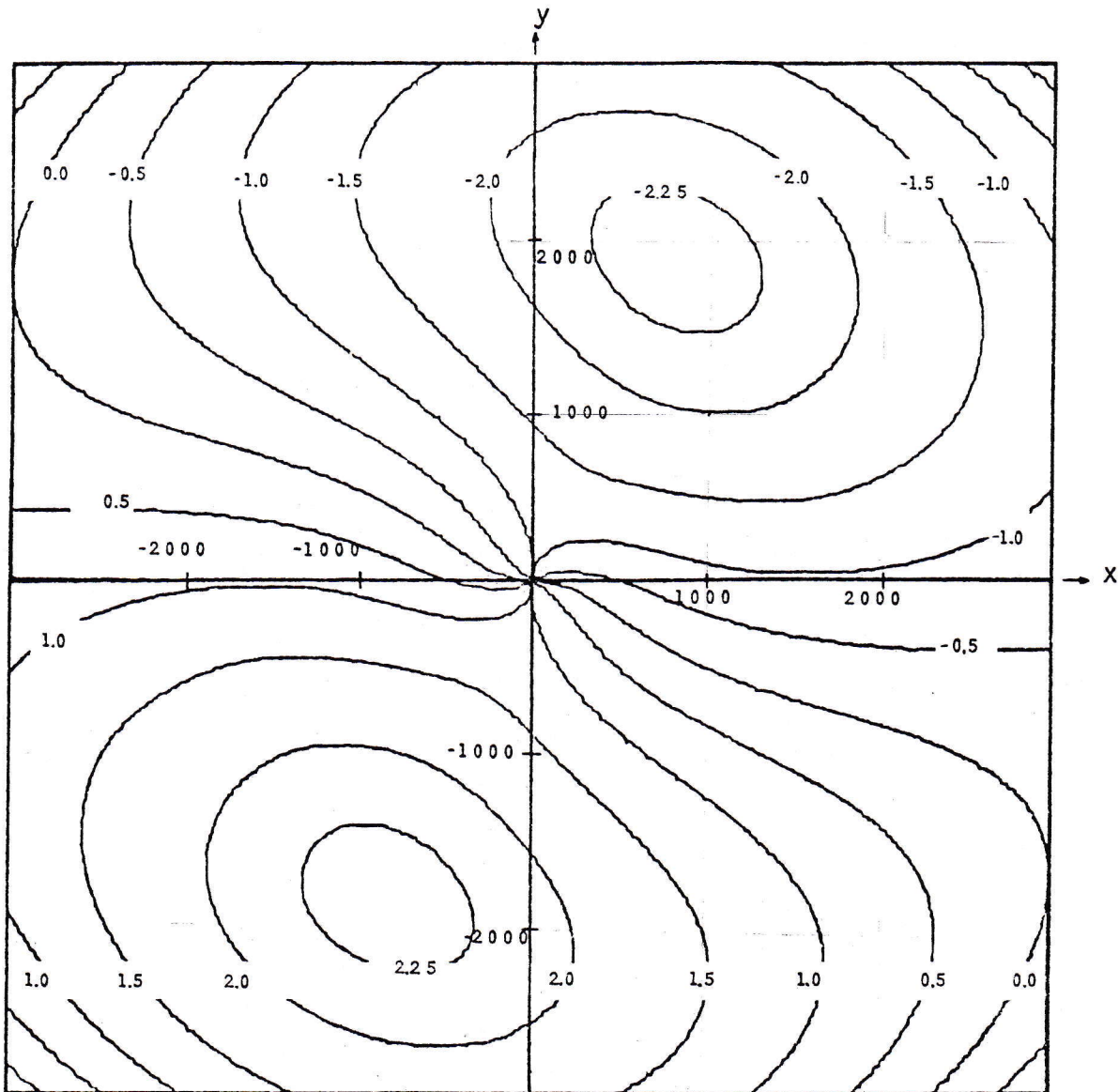
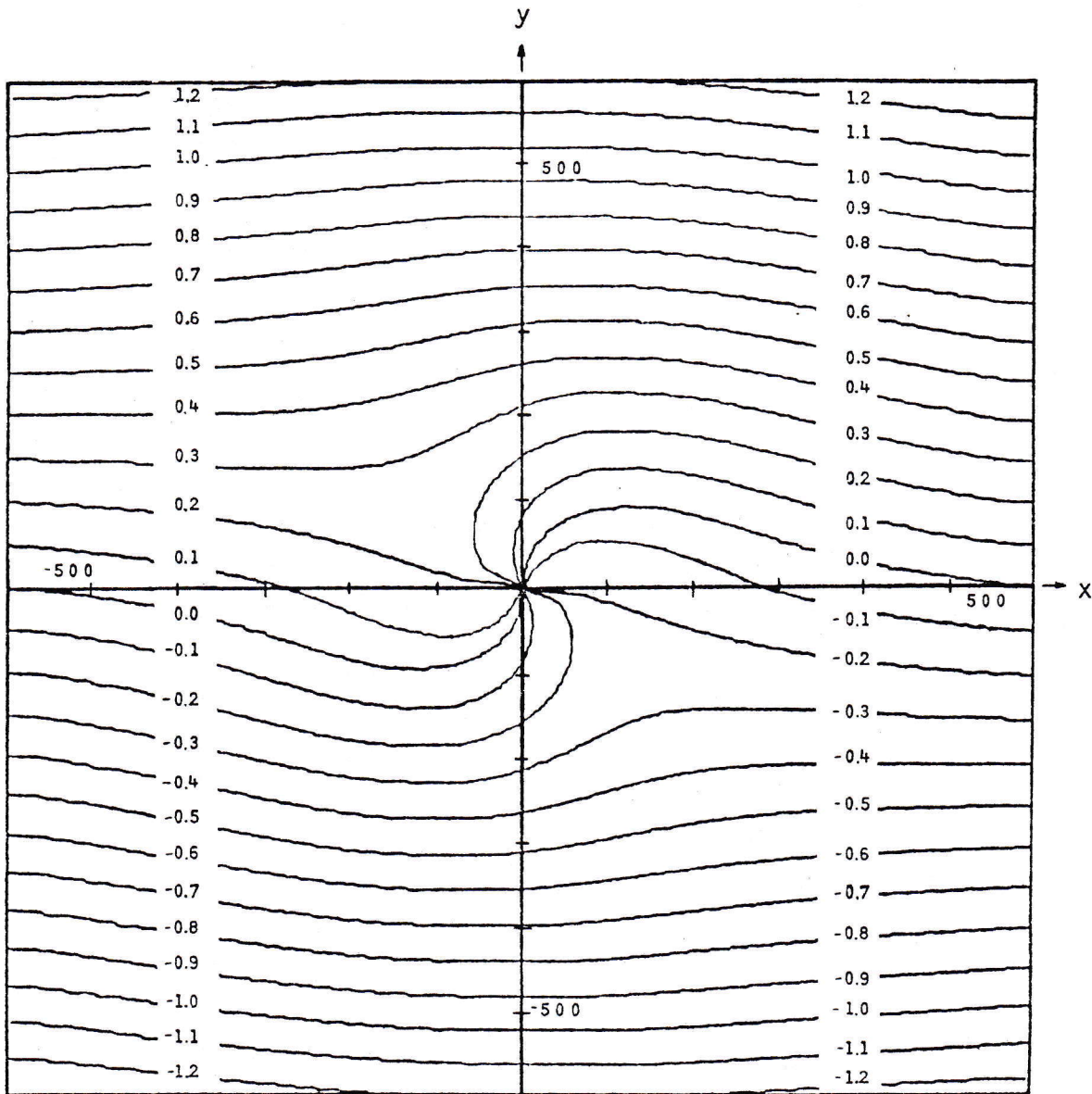


Figure 9.2 \dot{Y} Rendezvous Contours at $\dot{r}_{avg} = 1.0$

250 nm Circular Orbit

Figure 10.1 \dot{X} Rendezvous Contours at $\dot{r}_{avg} = 0.2$

250 nm Circular Orbit

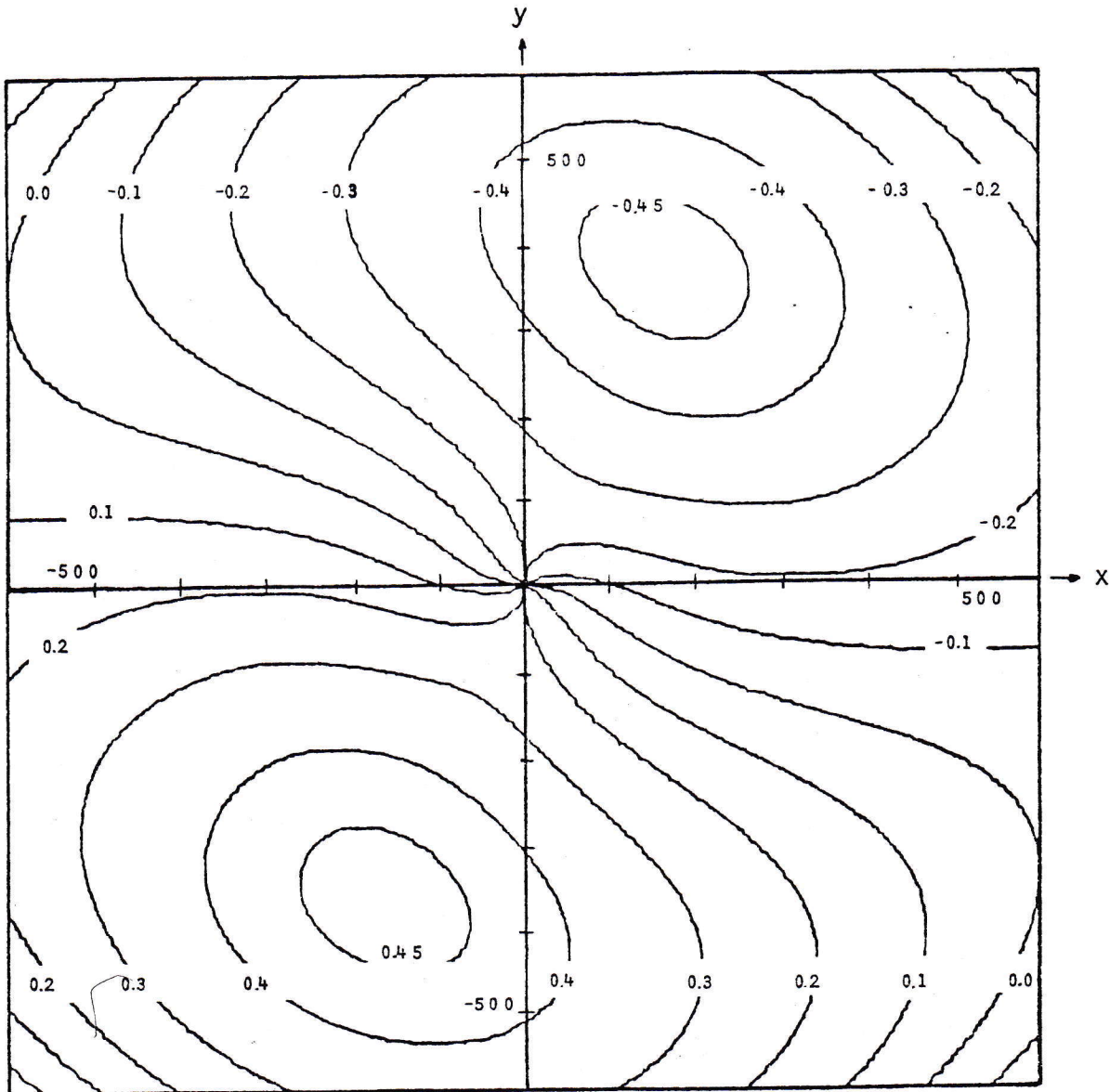


Figure 10.2 \dot{Y} Rendezvous Contours at $\dot{r}_{avg} = 0.2$

plots from $\dot{r}_{AVG} = 1.0$ unit/sec to any desired closure rate. This procedure, as well as general use of the contour plots is described through a series of example cases.

Case I

The space shuttle is 1000 meters directly ahead of a satellite to be retrieved. A rendezvous is required which will have an average closure rate of 1.0 meters/second (mps). The shuttle pilot, using Figures 9.1 and 9.2 (they are nondimensional), locates the relative position (-1000,0) on the contour plots. He reads off the necessary relative velocities for rendezvous and finds them to be $\dot{X} = 0.678$ mps and $\dot{Y} = 0.847$ mps.

Case II

An astronaut 1000 ft behind and 1000 ft above a space station wishes to return at a rate of 1.0 fps. Again using Figures 9.1 and 9.2, he locates his position (1000,1000) relative to the desired rendezvous point and then reads off the necessary X and Y components. He finds them to be $\dot{X} = 1.220$ fps and $\dot{Y} = -2.030$ fps.

Case III

The shuttle is 500 ft directly behind a satellite to be retrieved. A rendezvous with an average closure rate of 0.2 fps is desired. The 1.0 unit/sec contour plots may be used since the only difference between plots for different closure rates is a scaling factor determined by the ratio of the closure rates. The shuttle location on the $\dot{r}_{AVG} = 1.0$ contour plot is computed to be $X = 2500$ ($\frac{\dot{X}}{\dot{r}_{AVG}} = \text{CONST} \Rightarrow \frac{500}{.2} = \frac{X}{1} \Rightarrow X = 2500$)

and $Y = 0.0$ ($0./0.2 = Y/1. \Rightarrow Y = 0.$). Using Figures 9.1 and 9.2, the necessary relative velocity for this location (2500,0) is determined to be $\dot{X} = -.076$ fps and $\dot{Y} = -.857$ fps. Multiplying these values once again by a ratio of the closure rates, the necessary components for rendezvous at 0.2 fps are determined to be $\dot{X} = -.015$ fps ($\frac{\dot{X}}{r_{AVG}} = \text{CONST} \Rightarrow \frac{.076}{1} = \frac{\dot{X}}{.2}$) and $\dot{Y} = -0.171$ fps [$(\dot{Y} = 0.2)(-0.857)$]. It can be seen from Figures 10.1 and 10.2 that these are the correct values.

It should be noted that a singularity exists in eqs. 25 at

$\frac{R_0}{r_{AVG}} = 7922$. At this value, both \dot{X} and \dot{Y} go to infinity. This is

caused when the denominator $[8 \tan(\lambda) - 6\lambda]$ tends to zero.

$$8 \tan(\lambda) - 6\lambda = 0$$

$$\lambda^{-1} \tan(\lambda) = .75$$

$$\lambda \cong 4.419371$$

recall $\lambda = \frac{R_0 \omega}{r_{AVG}^2}$

so, for a 250 nm circular orbit

$$\left(\frac{R_0}{r_{AVG}} \right)_{\text{CRIT}} \cong 7921.661765$$

The critical radius for $\dot{r}_{AVG} = 0.2$ fps is then 1584.33 ft. Therefore, results of Equations (25) will not give accurate rendezvous from distances greater than 1584 ft (at $\dot{r}_{AVG} = 0.2$ fps). At smaller \dot{r}_{AVG} values, the range limitation of this rendezvous technique continues to decrease. For a range of 1000 ft, the critical \dot{r}_{AVG} is 0.12624 fps. However, this

is not a physical limit, but a result of the linearization of the equations of motion. Since all further analysis will concentrate on small values of $\frac{R_0}{\dot{r}_{AVG}}$ (where linearization methods give very high accuracy), this mathematical singularity will not be considered further.

This generalized rendezvous technique may now be applied to the problem of shuttle proximity operations. Figures 11.1 and 11.2 depict \dot{X} and \dot{Y} contours at ranges of 1200 ft from the target point for an \dot{r}_{AVG} rate of 1.0 fps. A range of 1200 ft was chosen since NASA is currently considering stationkeeping points within this range. An average closure rate of 1.0 fps is presented since it is easily converted to any other desired closure rate. It must be noted that the \dot{r}_{AVG} value is simply an average closure rate found by dividing the initial distance by the coast time (Eq. 22). In general, it does not accurately represent the final closure rate. This property is shown in Figure 12 and 13 where the initial velocities required for rendezvous as well as the final closure velocities for \dot{r}_{AVG} rates of 0.2 fps (Figure 12) and 1.0 fps (Figure 13) are plotted against θ , the initial position angle

($\cos\theta = \frac{X_0}{R_0}$; $\sin\theta = \frac{Y_0}{R_0}$). For all cases, the initial distance (R_0) was 1000 ft. Several interesting results become apparent when studying these figures. First, at stationkeeping points on the X axis

($\theta = 90^\circ, 270^\circ$), the initial and final velocities for the $\dot{r}_{AVG} = 0.2$ fps rendezvous are both less than 0.2 fps while the corresponding values for $\dot{r}_{AVG} = 1.0$ fps rendezvous are greater than 1.0 fps. Secondly, from stationkeeping points on the Y axis ($\theta = 0^\circ, 180^\circ$), the initial and

$\dot{r}_{avg} = 1.0$
250 nm Circular Orbit

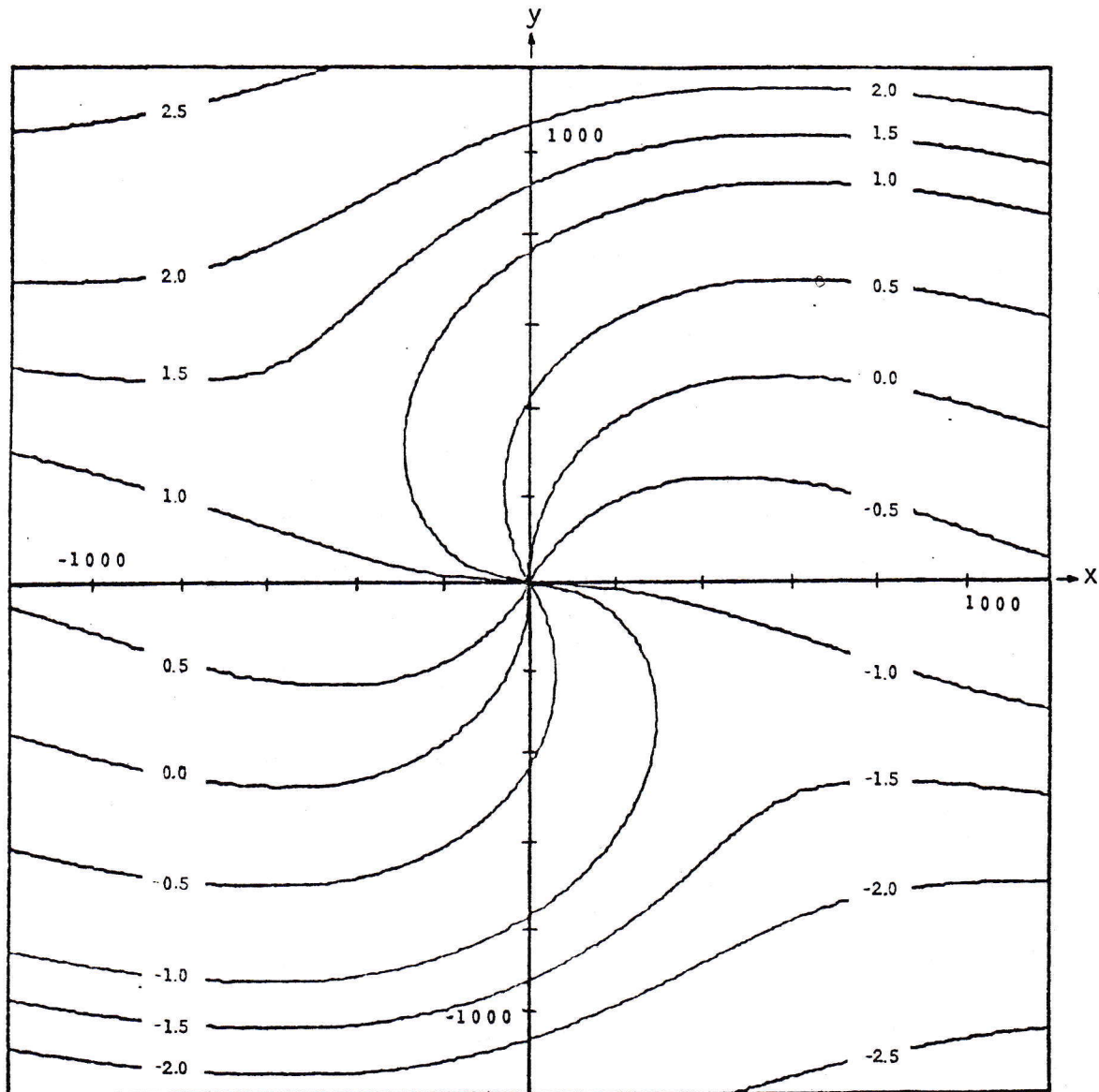


Figure 11.1 Local \dot{X} Rendezvous Contours

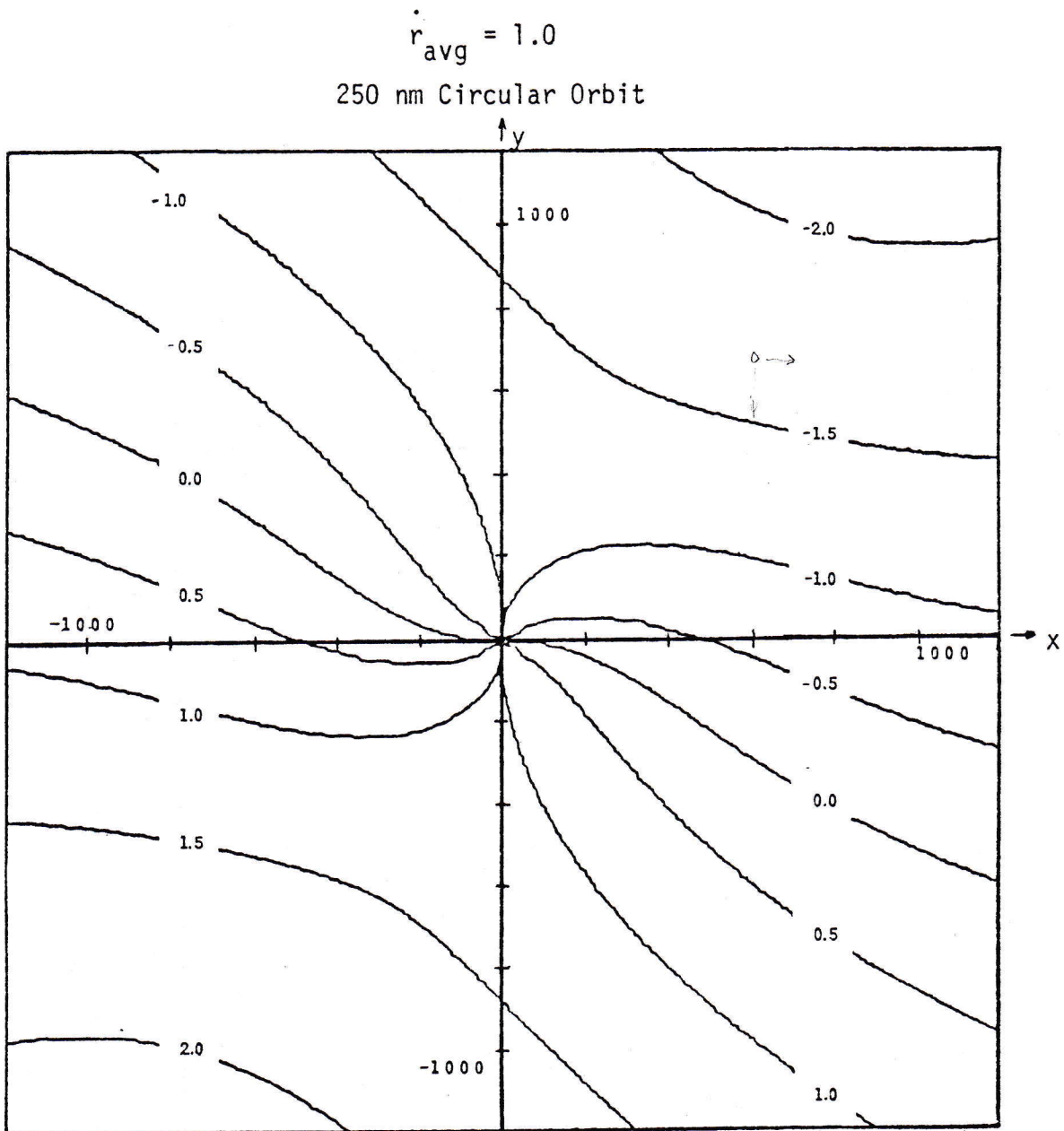


Figure 11.2 Local \dot{Y} Rendezvous Contours

$\dot{r}_{avg} = 0.2 \text{ fps}$
 $r_{S/T} = 1000 \text{ FT}$

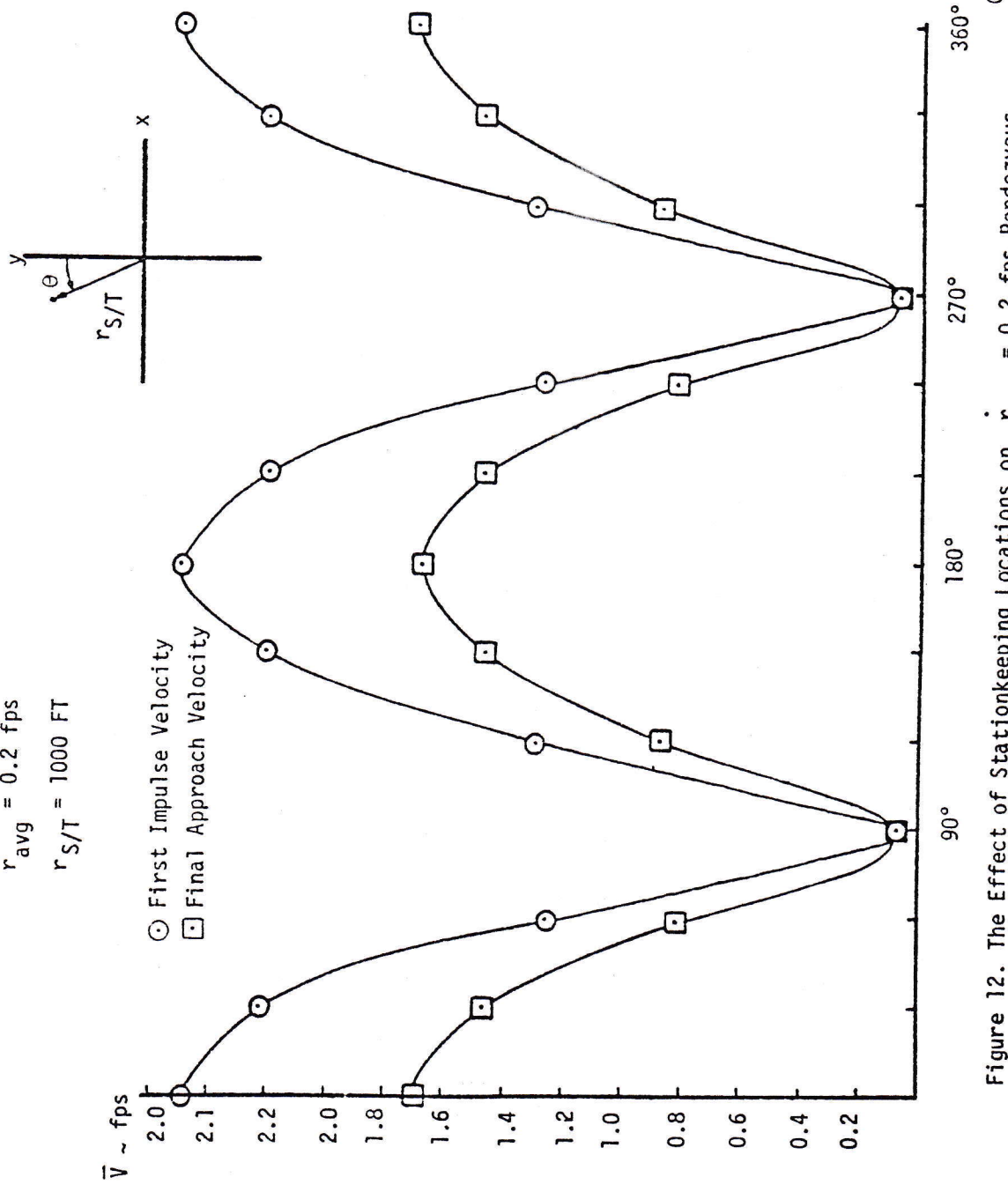


Figure 12. The Effect of Stationkeeping Locations on $\dot{r}_{avg} = 0.2 \text{ fps}$ Rendezvous Trajectories

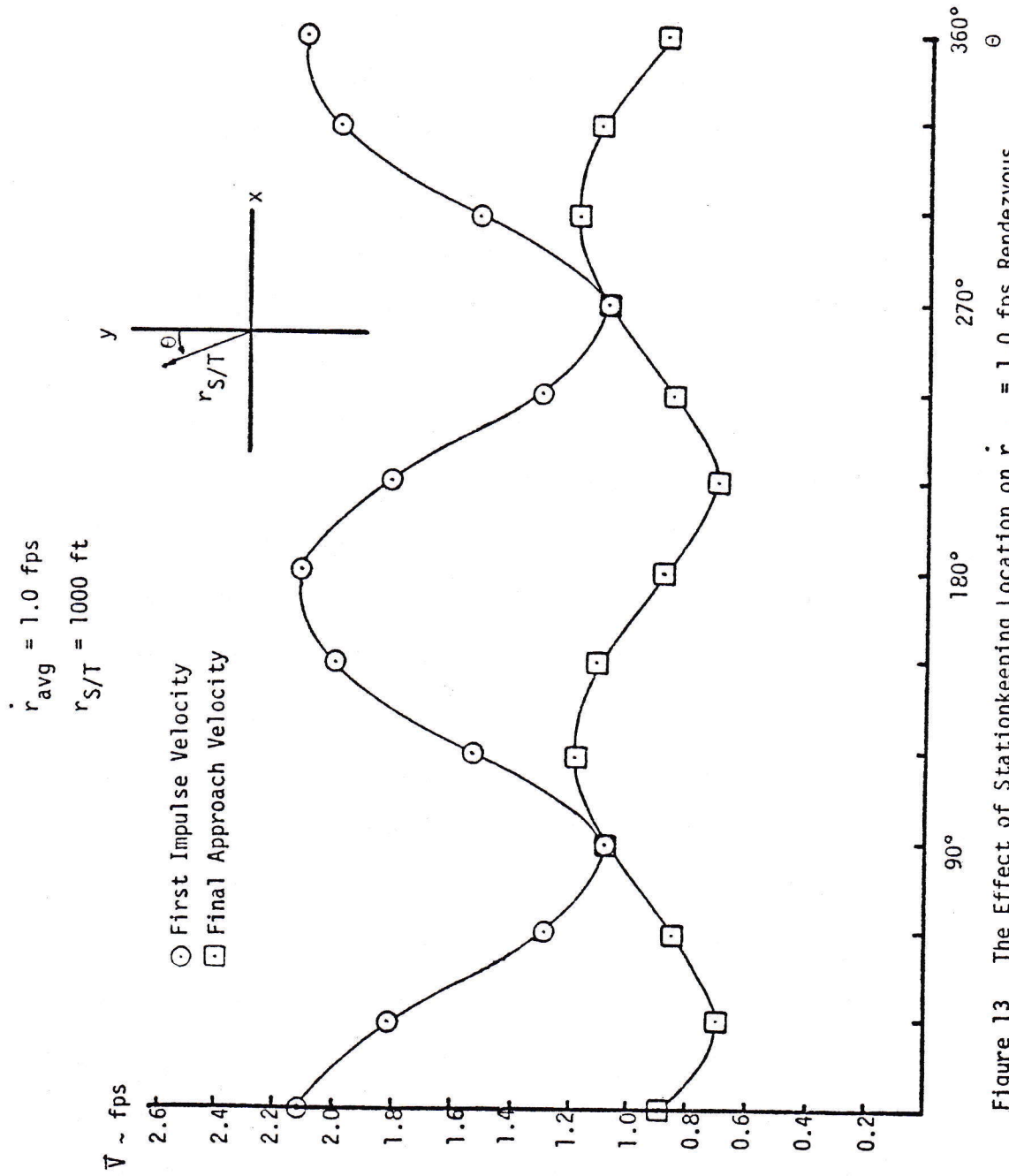


Figure 13 The Effect of Stationkeeping Location on $\dot{r}_{avg} = 1.0 \text{ fps}$ Rendezvous Trajectories

final velocities for $\dot{r}_{AVG} = 0.2$ fps rendezvous are both considerably greater than 0.2 fps while for $\dot{r}_{AVG} = 1.0$ fps rendezvous, the initial velocity is about 2.12 fps yet the final closure rate is about 0.85 fps. Due to this complex behavior it is not possible to easily relate average closure velocity and final closure rate using this rendezvous method.

Another rendezvous technique suggested by Mueller⁵ is the straight line approach. Using this method, the shuttle would establish a line-of-sight motion directly toward the target point. Any ensuing motion off of the initial line-of-sight would be negated at either regular time intervals or when the magnitude reached a predetermined level. For simulation purposes, a closure rate of 1.0 fps was established. Corrections were made at intervals of 100 seconds. The magnitude of the velocity correction was double that of the accumulated velocity away from the original line-of-sight and opposite in direction. The corrective velocity was doubled in magnitude so that a velocity component back to the original line-of-sight was established.

Henceforth, the Mueller linear approach will be referred to as the line-of-sight approach. Also, all rendezvous made using the contour plots of Equation (25) will be referred to as chart-directed trajectories. Figures 14.1 to 14.5 denote line-of-sight and chart directed ($\dot{r}_{AVG} = 0.2$ fps and $\dot{r}_{AVG} = 1.0$ fps) rendezvous trajectories from locations 1000 ft away in directions 1 through 5 as defined in Figure 2. For example, the coordinates of a point 1000 ft away in direction 2 would be (707,707); for direction 5 they would be (0,-1000). Trajectories from $Y = -1000$ ft (direction 5) are presented in addition to $Y = +1000$ ft (direction 1)

for reasons which will become apparent when reading the next chapter.

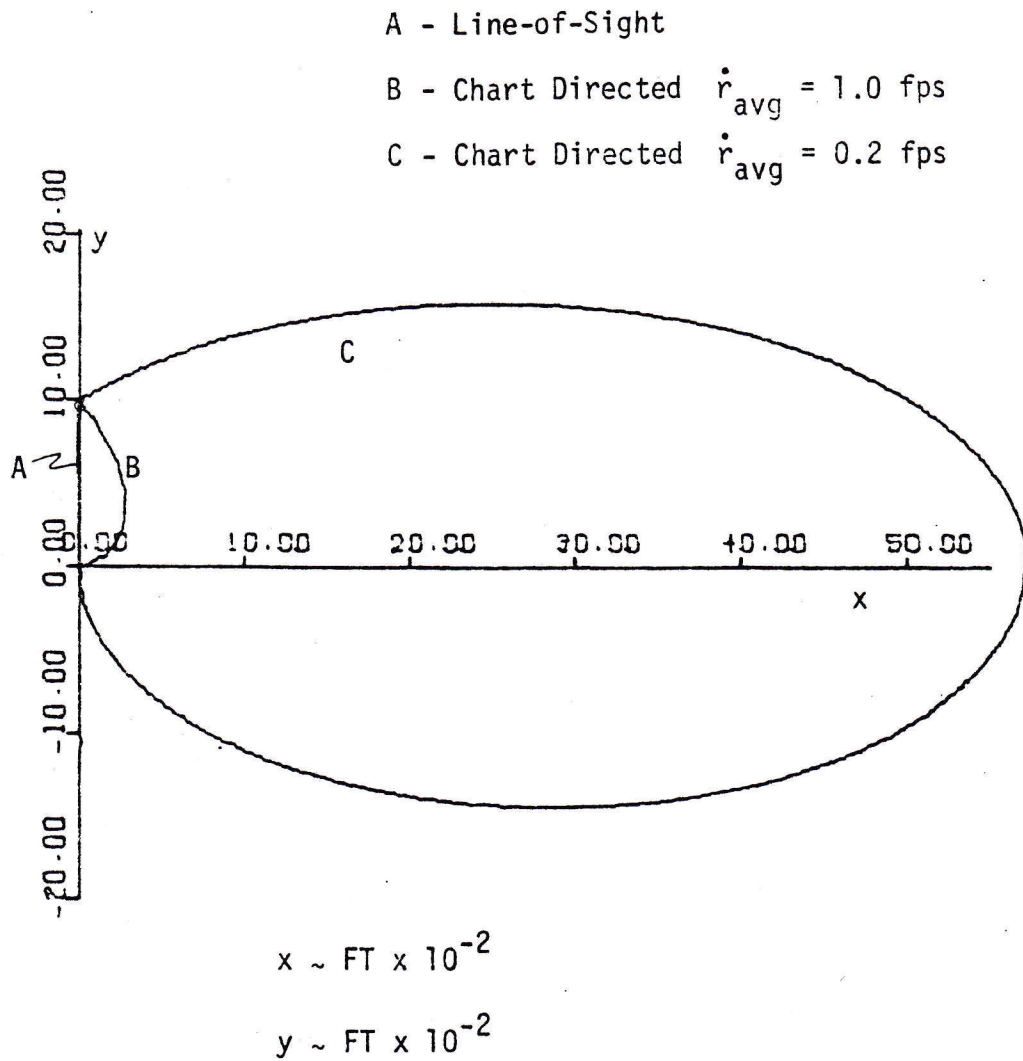
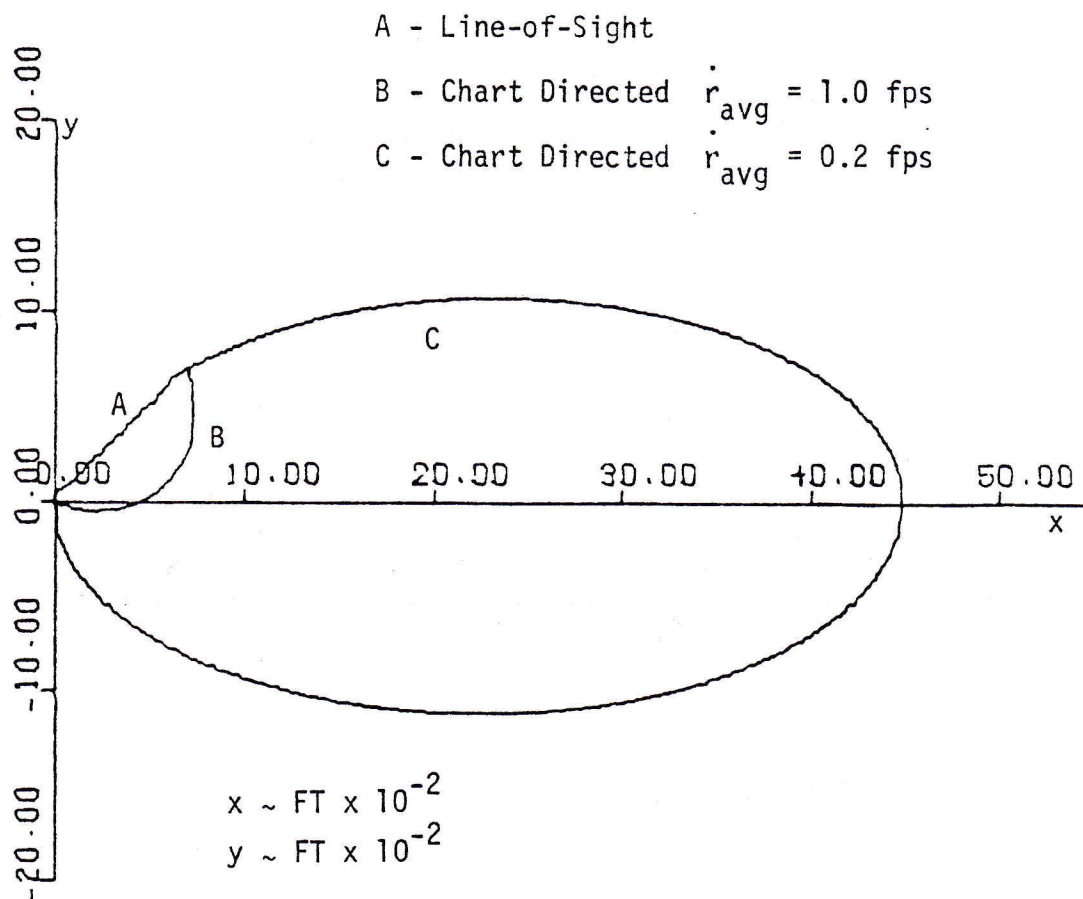


Figure 14.1 Rendezvous Trajectories from $Y = 1000$ FT



Figures 14.2 Rendezvous Trajectories from $X = Y = 707$ FT

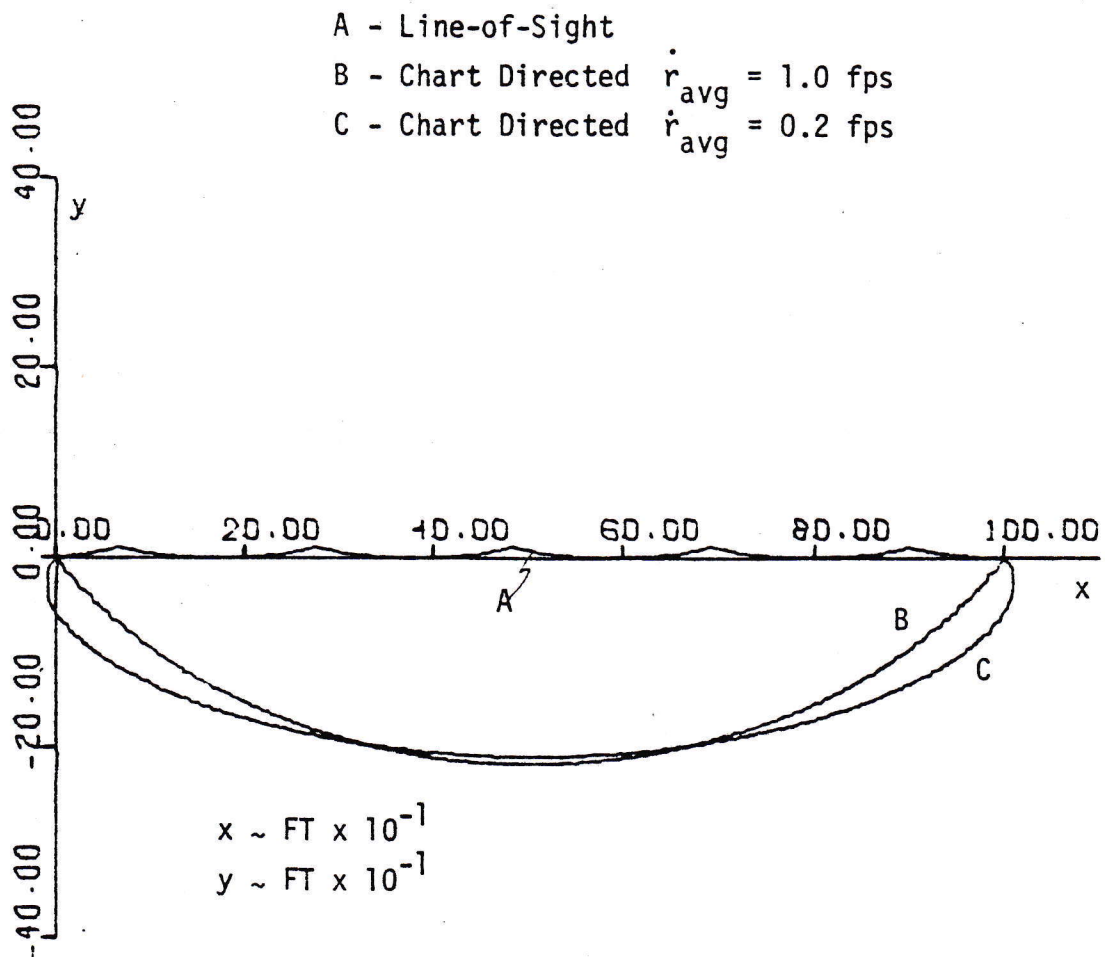


Figure 14.3 Rendezvous Trajectories from X = 1000 FT

A - Line-of-Sight

B - Chart Directed $\dot{r}_{avg} = 1.0$ fps

C - Chart Directed $\dot{r}_{avg} = 0.2$ fps

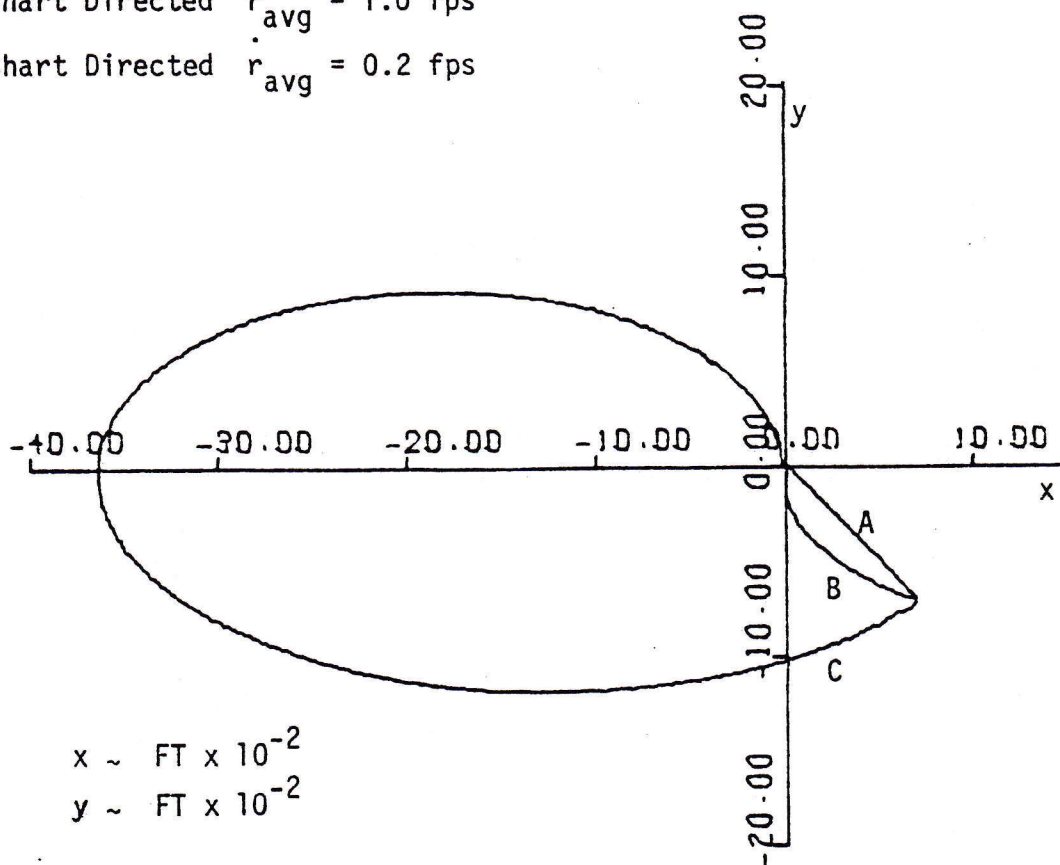


Figure 14.4 Rendezvous Trajectories from $X = -Y = 707$ FT

A - Line-of-Sight

B - Chart Directed $\dot{r}_{avg} = 1.0$ fps

C - Chart Directed $\dot{r}_{avg} = 0.2$ fps

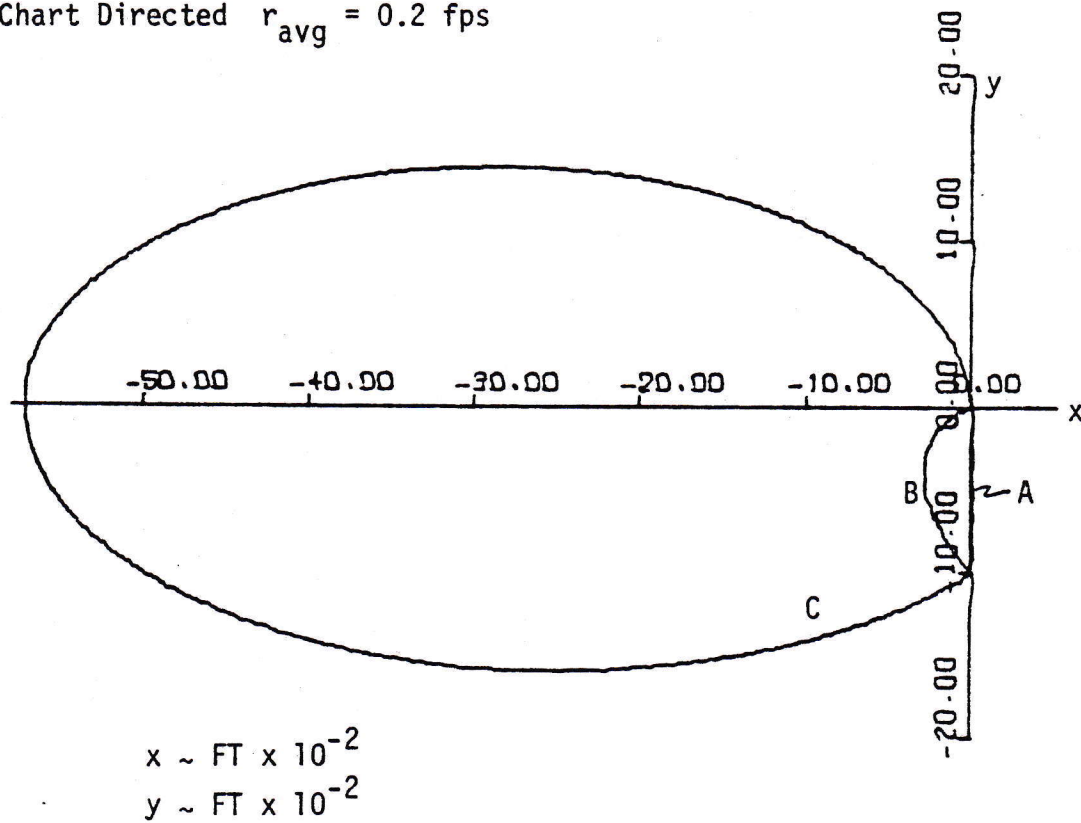


Figure 14.5 Rendezvous Trajectories from $Y = -1000$ FT

CHAPTER 6

Trajectory Optimization

NASA has recently studied two inplane rendezvous trajectories for shuttle proximity operations. The first of these trajectories, denoted \bar{V} , (V-bar) utilizes stationkeeping points along the orbital velocity vector of the target point. This would correspond to locations directly in front or behind the target point; or, points along the $\pm X$ axis of the coordinate system previously defined in this text. The second trajectory under study, denoted \bar{R} , (R-bar) employs stationkeeping points along an earth radius vector through the target point. In the (X,Y,Z) system, this corresponds to locations directly above and below the origin ($\pm Y$ axis). For this reason, these stationkeeping points are not stable. Both proposed trajectories are straight line approaches with initial relative distances of 1000 ft. Hence, the \bar{V} approach would be along the orbital velocity vector (\bar{V}) of the target body. The \bar{R} approach would be along an earth radius vector (\bar{R}) through the target body. The line-of-sight Mueller approach as described in Chapter 5 is a very close approximation to these trajectories and will be used as a basis of comparison in the remainder of this chapter. Due to similarities between the rendezvous trajectories from position 3 and 7 and since NASA has considered \bar{R} approaches from below the target point, only stationkeeping locations of (1000,0) ft and (0, -1000) ft will be presented. These correspond to directions 3 and 5 respectively.

Rendezvous trajectories from these two stationkeeping locations have been previously analyzed using the line-of-sight and the chart directed techniques. These results are documented in Figures 14.3 and 14.5, Chapter 5. Other possible trajectories become apparent when reviewing results of the negative time integration (Figure 3, Chapter 3, and Figure 7, Chapter 4). It can be seen from these figures that the stationkeeping (X or Y axis crossing point) distance is linearly related to the relative velocity at the target point. Hence, it can also be seen from Figures 3 and 7 that trajectories from $X = 1000$ ft would have a final relative velocity less than 0.2 fps (one impulse) unless the final approach is from directly below. This case is presented in Figures 3.1 and 7.1 and would be a two impulse trajectory.

Likewise, all approaches from $Y = -1000$ ft would require two impulses. Rendezvous trajectories from both of the X and Y stationkeeping locations are presented in Figures 15.1 and 15.2 respectively. Also, a summary of parameters of all possible rendezvous trajectories (as shown in Figures 14.3, 14.5, 15.1, and 15.2) is presented in Table I.

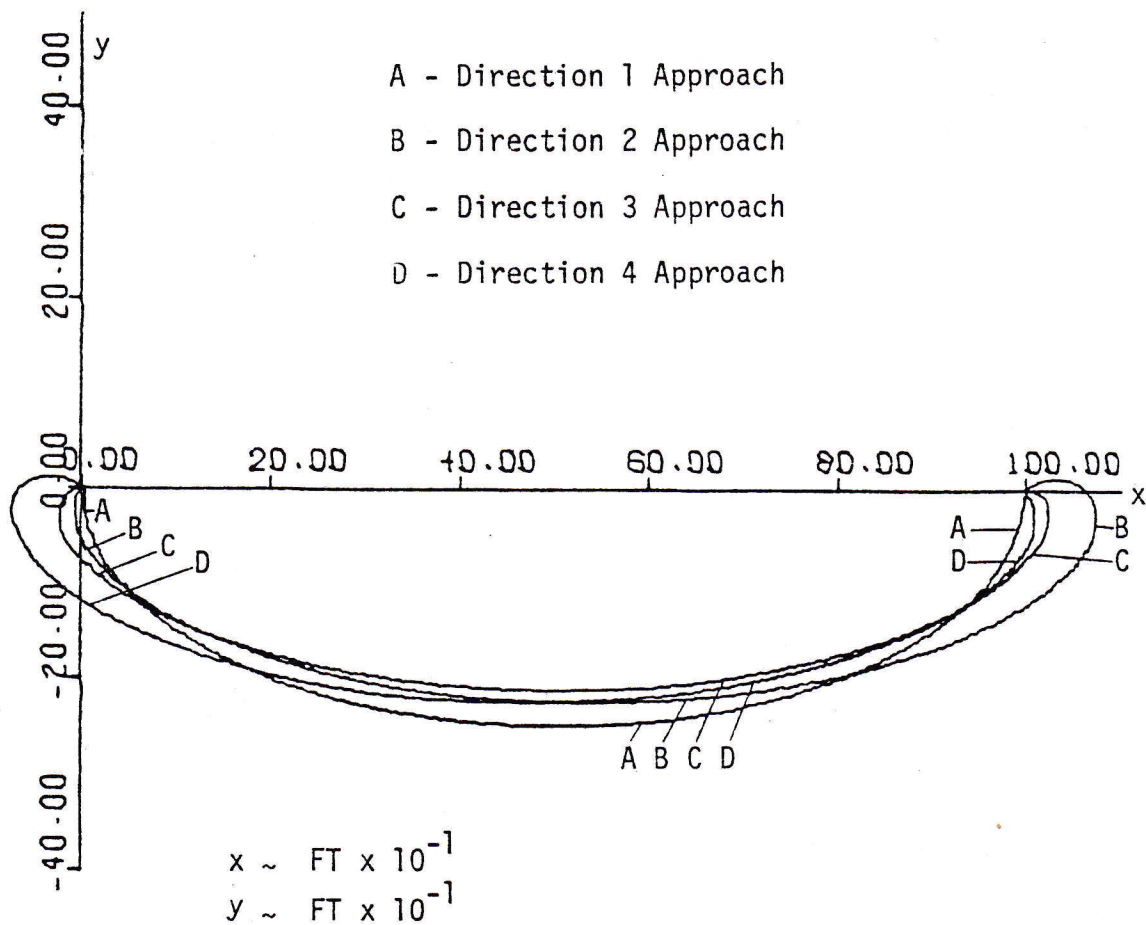


Figure 15.1 Negative Time Integration Rendezvous Trajectories from
X = 1000 ft

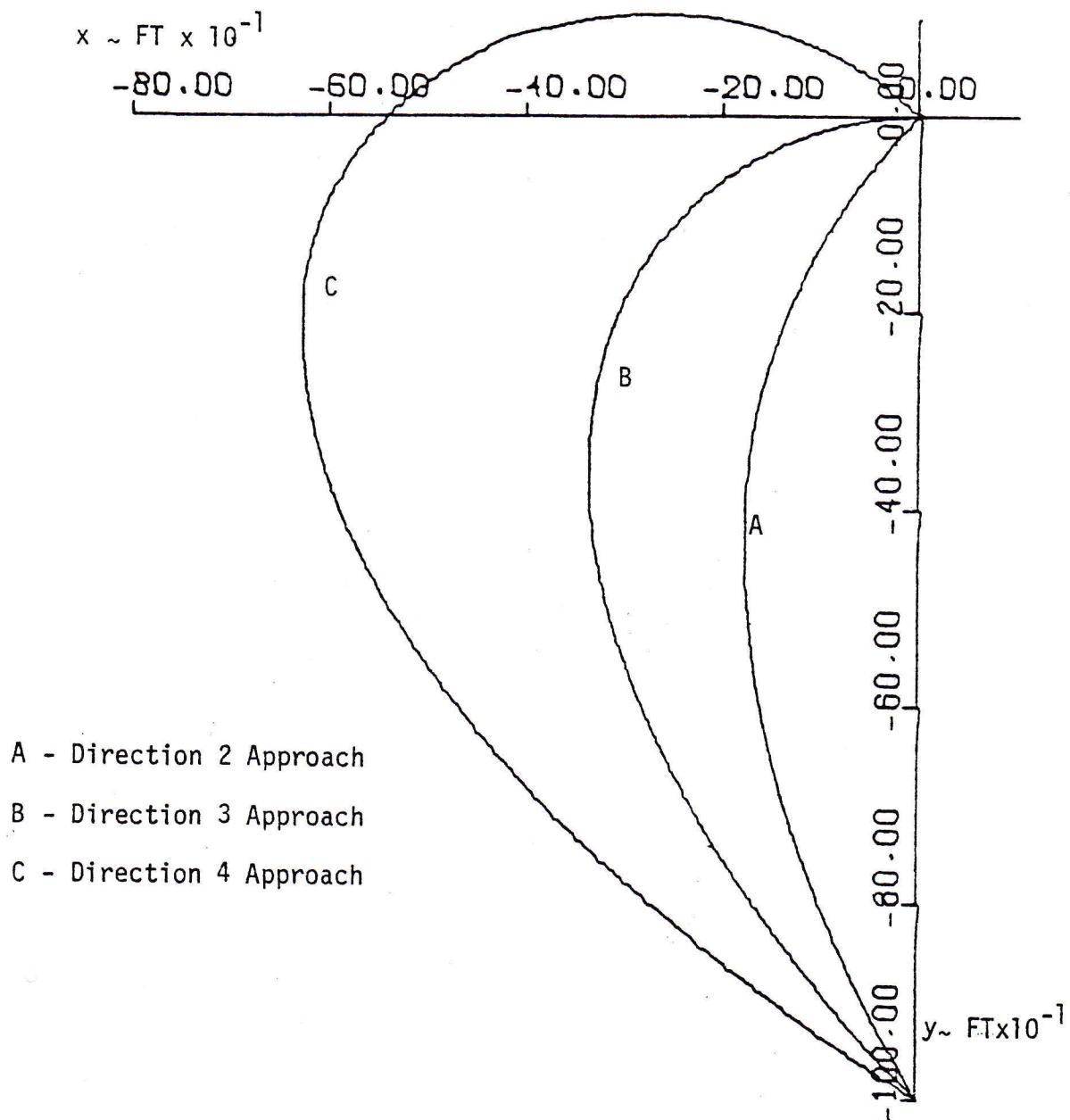


Figure 15.2 Negative Time Integration Rendezvous Trajectories
from $Y = -1000 \text{ FT}$

TABLE I
Summary of Rendezvous Trajectory Parameters

Rendezvous Procedure	Notes	Stationkeeping Location		First Impulse		Approach Velocity		Coast Time ~sec.	Total ΔV^* ~ft/sec.
		x	y	\dot{x}	\dot{y}	\dot{x}	\dot{y}		
Line-of-sight Approach	11 ¹	1000	0	-1.0	0	-.997502	-.070610	1008.	4.116258
	11	0	-1000	0	1.0	.103002	1.006700	992.	5.165330
Chart-Directed Approach	1.0 ²	1000	0	-0.678385	-0.846632	-.678317	.846687	1000.	1.969786
	1.0	0	-1000	-1.384905	+1.602521	.846487	.185234	1000.	2.784543
	0.2	1000	0	0.056706	-0.041678	.053911	.045292	4970.	0.070375**
	0.2	0	-1000	-2.189860	-1.343707	.041864	-1.692375	5000.	4.062141
Negative Time Integration Approach	1 ³	1000	0	0.059346	0	0.059344	0.000046	5628.	0.059346**
	2	1000	0	0.059346	0.059346	0.058865	0.059823	5628.	0.083928**
	3	1000	0	0	-0.278940	0	0.278940	2815.	0.357880***
	4	1000	0	0.059346	-0.059346	0.059337	-0.059355	5631.	0.083928**
	2	0	-1000	-1.239881	+2.040672	+0.991524	+0.992003	632.	3.590378
	3	0	-1000	-1.444951	+1.505246	+0.786888	+0.000022	1143.	2.673428
	4	0	-1000	-1.736332	+1.100263	+0.495928	-0.495003	1925.	2.556279

¹Total number of impulses

²r² AVG

³Direction of final approach

* ΔV = Magnitude of first impulse plus required magnitude of second impulse (if needed) to reduce approach velocity to 0.2 fps.

**One impulse trajectory

***Periodic trajectory

Optimality

In determining the optimum shuttle rendezvous trajectory, there are six parameters to be considered.

- (1) total ΔV required,
- (2) initial stationkeeping location,
- (3) coast time,
- (4) crew visibility,
- (5) plume impingement, and
- (6) general safety

There are no hard constraints on coast time. However, a reasonable maximum allowable time might be one orbital period (5631 seconds for a 250 nm orbit). Due to the large number of tasks which may need to be accomplished while enroute (shuttle systems checks, RMS checkout procedures, payload checklists, monitoring of the trajectory), it is not desirable to have a very short coast time. The total ΔV required to achieve a rendezvous (with less than 0.2 fps relative velocity) should be kept to a minimum. Constraints on crew visibility and plume impingement have been mentioned previously. The initial stationkeeping location should be far enough away to insure that no plume impingement will occur from the first impulse, yet remain within 1000 ft of the target point. Finally, the general safety of the rendezvous procedure should be adequate. That is, the rendezvous should be easily initiated (no intricate shuttle attitude or complex velocity components required), amenable to midcourse corrections if needed (for accuracy of final approach), and easily discontinued without damage to the shuttle or target body.

Three rendezvous techniques have been developed. Data used in the following discussion concerning these methods is taken from Table I.

Rendezvous Trajectories from $Y = -1000$ ft Stationkeeping Location

A. Line-of-sight approach (Figure 14.5, Chapter 5)

A line-of-sight approach from $Y = -1000$ ft (from below the target) constitutes a multi-impulse trajectory with a coast time of 1000 seconds. It is a good approximation to the \bar{R} approach. Crew visibility as well as general safety of this approach is excellent, however, an excessive amount of fuel is used ($\Delta V = 5.165$ fps). Also, since this maneuver is not a one impulse approach, plume impingement considerations would be necessary. Line-of-sight approaches from this position with smaller closure rates consumed comparable amounts of fuel despite the increase in coast time.

B. Chart directed approach (Figure 14.5, Chapter 5)

The $\dot{r}_{AVG} = 0.2$ fps chart directed approach from $Y = -1000$ ft requires large initial and final impulses. The ΔV requirements for this case are very large and are indeed greater than for the same approach at $\dot{r}_{AVG} = 1.0$ fps (see Table I). Due to the necessity of a second impulse, plume impingement considerations are necessary. Crew visibility can only be maintained by rotating the shuttle enroute. The general safety is minimal due to complex shuttle attitudes and the long (5000 sec.) coast time involved. Also, the entire trajectory is very sensitive to initial ΔV errors (direction or magnitude), and accuracy would be difficult to maintain while rotating the shuttle.

The chart directed trajectory at $\dot{r}_{AVG} = 1.0$ fps from $Y = -1000$ ft has a coast time of 1000 seconds and exhibits a moderate ΔV requirement.

However, plume impingement effects must be considered due to a final relative velocity greater than 0.2 fps. Crew visibility may be adequately maintained by using a constant nose-forward shuttle attitude. General safety is adequate although complex initial velocity components are required.

C. Negative time integration (Figure 15.2)

No one impulse trajectories were found from $Y = -1000$ ft using the negative time integration procedure. The two impulse solutions identified have relatively short coast times and use a moderate amount of fuel (ΔV). Crew visibility is adequate from a constant nose-down attitude in all but one case (direction 4 approach). For this case, the shuttle would again need to be rotated enroute. Since all are two impulse maneuvers, plume impingement considerations are necessary. The general safety of these approaches is minimal due to the complex thrust components required and the short coast times involved. In general, the trajectories found using the negative time integration procedure are very similar to chart directed trajectories computed at comparable \dot{r}_{AVG} values.

Rendezvous Trajectories from $X = 1000$ ft Stationkeeping Location

A. Line-of-sight approach (Figure 14.3, Chapter 5)

A line-of-sight approach from $X = 1000$ ft (from behind the target) is very similar to the Y axes approach. It is also a good approximation to the \bar{V} approach. Total ΔV requirements are excessive ($\Delta V=4.116$ fps) yet coast time (for $\dot{r} = 1.0$ fps) and crew safety are excellent. Plume impingement considerations are necessary for \dot{r}_{AVG} rates greater than 0.2 fps. Once again, line-of-sight approaches at smaller \dot{r}_{AVG}

values displayed comparable ΔV requirements with associated increases in coast time.

B. Chart directed approach (Figure 14.3, Chapter 5)

The chart directed approach from $X = 1000$ ft at $\dot{r}_{AVG} = 0.2$ fps is interesting due to its extremely small ΔV requirement. Data from this study indicates that the shuttle will remain within capture distance for approximately 18 minutes with a relative velocity of about 0.08 fps. However, the coast time involved is 5000 seconds and it is doubtful if crew visibility can be maintained from a constant shuttle attitude while enroute. General safety is adequate; however, the intricate initial velocity components as well as the small velocity magnitude (15 second "burn" with one 25 lbf VRCS thruster) and long coast time makes the accuracy of this trajectory very difficult to attain.

The chart directed approach from $X = 1000$ ft at $\dot{r}_{AVG} = 1.0$ fps is a two impulse maneuver with a coast time of 1000 seconds. Again, plume impingement considerations are necessary. Total ΔV requirements are moderate ($\Delta V = 1.970$ fps) and crew visibility is adequate from a constant nose-down shuttle attitude. The general safety is adequate yet complex initial velocity components are required.

C. Negative time integration (Figure 15.1)

Four rendezvous trajectories are apparent when studying the negative time integration results for stationkeeping points at $X = 1000$ ft. Three of these trajectories are one impulse trajectories and are similar to the chart directed approaches but have a longer coast time (5631 seconds). These trajectories also display poor visibility but excellent ΔV requirements. The fourth of these trajectories (two impulse) has a shorter coast time (2815 sec), a moderate ΔV requirement, and ex-

cellent crew visibility characteristics in a nose-down constant shuttle attitude. This maneuver is easily initiated (thrust along a radius vector toward the earth), and relatively amenable to midcourse maneuvers. Plume effects would be easily minimized due to the relative motion of the two bodies during final rendezvous. Also, if allowed to do so, the trajectory would return the shuttle to its original stationkeeping location with no further thrust. Another version of this same periodic trajectory would be the one impulse case ($\bar{V}_0 = 0.2$ fps) starting from a stationkeeping point at $X = 717$ ft (Figure 7.1). This would offer the same benefits as the previously periodic rendezvous trajectories yet reduce the ΔV required and eliminate all plume impingement considerations. A third alternative is a combination of these two techniques. That is, a series of two one-impulse trajectories could be used to achieve a final closure rate of 0.2 fps or less. The approach would initiate at $X = 1000$ ft and the first segment of the approach would take the shuttle to $X = 500$ ft. At this point, all motion would be stopped and the second segment of the approach would be initiated. It may be determined (by techniques to be described) that the magnitude of the first impulse must be $-.14$ fps to take the shuttle on a periodic trajectory to $X = 500$ ft. The second impulse would then be $-.28$ fps to negate all previous relative velocity and establish a second "hop" to the target point. The coast time for such a two "hop" trajectory would be one orbital period, or 5631 seconds for a 250 nm circular orbit.

A method for determining the necessary \dot{Y} velocity ($\dot{X} = 0$) to affect a periodic rendezvous from any X axis stationkeeping loca-

tion is now described. The existence of such a relationship is suggested by Figure 3.1, Chapter 3 and Figure 7.1, Chapter 4. A correlation may be drawn between these periodic trajectories and the chart directed trajectories described in Chapter 5. It is known that all the periodic trajectories have a transfer time of one-half orbital period. Thus, by dividing the original distance (X coordinate) by this coast time, a specific \dot{r}_{AVG} value may be determined for any X axis stationkeeping location. It follows that for $\dot{r}_{AVG} = 1.0$ fps, the \dot{X} component should go to zero at $X = 2815.63$ ft (one half orbital period \times 1.0 fps). This may be verified by Figure 9.1, Chapter 5. The \dot{Y} component at this point ($X = 2815.63$ ft, $\dot{r}_{AVG} = 1.0$ fps) is found to be -0.7854 fps. The necessary \dot{Y} velocity component for a periodic rendezvous from any other X axis stationkeeping location is defined by a ratio of the \dot{r}_{AVG} closure rates. For example, a periodic rendezvous from $X = 717$ ft would have an average closure rate given by:

$$\dot{r}_{AVG} = \frac{R_0}{t_r} = \frac{717}{2815.63} = 0.25465 \text{ fps.}$$

By ratioing these closure rates, the necessary \dot{Y} velocity may be found.

$$\frac{\dot{r}_{AVG} 717}{\dot{r}_{AVG} 2815} = \frac{\dot{Y}_{717}}{\dot{Y}_{2815}} == \frac{.25465}{1} = \frac{\dot{Y}}{-0.7854}$$

$$\therefore \dot{Y}_{717} = -0.2 \text{ fps}$$

So, at $X = 717$ ft, a $\dot{Y} = -0.2$ fps thrust would be necessary for a periodic transfer to the target point. This result is verified by Figure 7.1, Chapter 4. The general relationship between stationkeeping location and \dot{Y} is given by:

$$\dot{Y} = (X)(-2.7894 \times 10^{-4})$$

In Figure 16, ΔV requirements are compared for line-of-sight approaches, chart directed rendezvous at $\dot{r}_{AVG} = 1.0$ fps and 0.2 fps, and for the periodic transfers described in the preceding paragraphs. Results are presented for both $X = \pm 1000$ ft and $X = \pm 717$ ft station-keeping locations. The other trajectories resulting from the negative time integration method are not presented due to their similarity to the chart directed maneuver. A drastic difference in the fuel requirements may be seen between the various rendezvous methods. For approaches from $X = \pm 1000$ ft, the line-of-sight trajectory is found to use the most fuel ($\Delta V = 4.116$ fps). The minimum amount is used by the chart directed $\dot{r}_{AVG} = 0.2$ fps trajectory ($\Delta V = .070$ fps). This represents a 98.3% reduction in fuel consumption. Similar results are noticed for the stationkeeping points at $X = \pm 717$ ft.

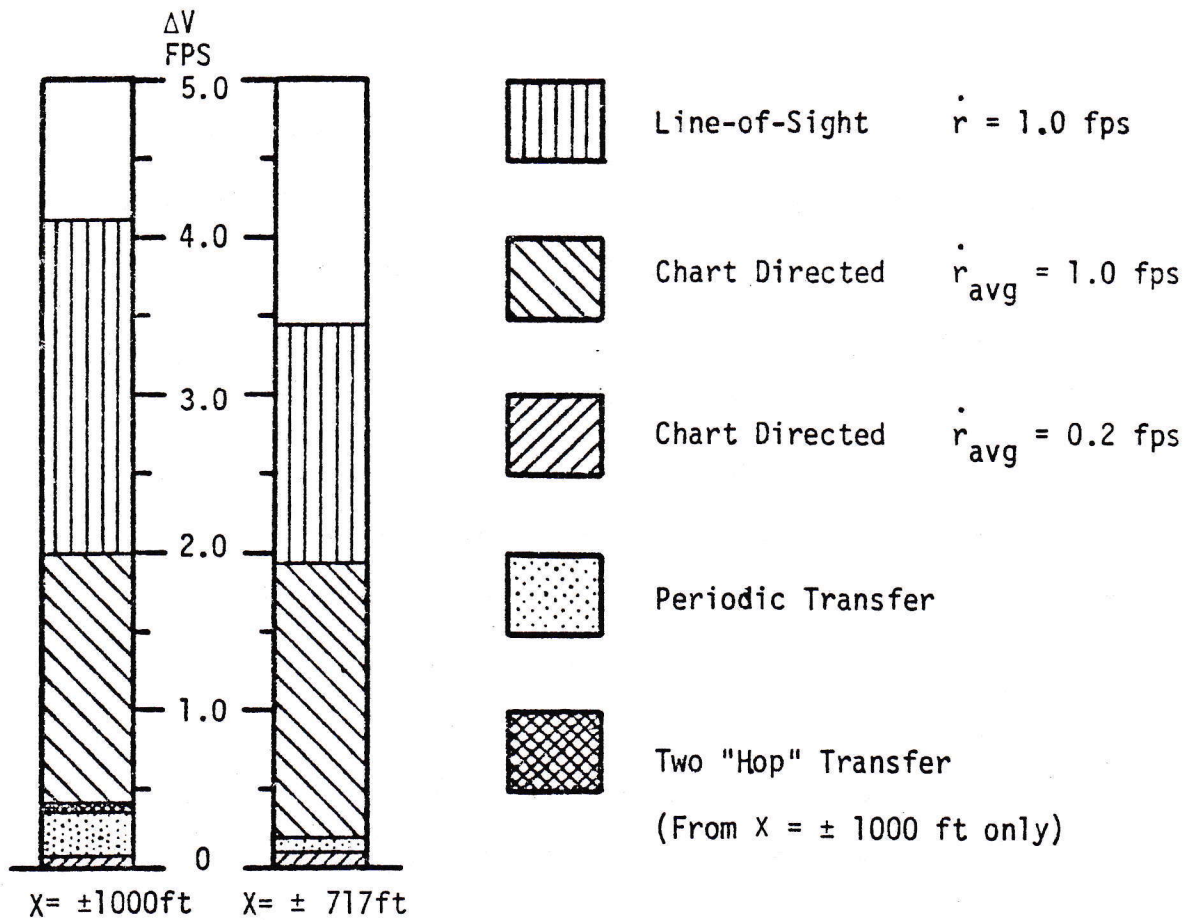


Figure 16 ΔV Requirements for Rendezvous from Stationkeeping Locations of $X = 1000$ FT and $X = \pm 717$ FT

CHAPTER 7

Conclusions and RecommendationsSummary

The Lagrangian method is used to derive the equations of motion for a body in near earth orbit. Three techniques for identifying possible shuttle-target point rendezvous are developed. They are:

- (1) Negative time integration,
- (2) Chart directed (equations developed by R. S. Dunning),
- (3) Line-of-sight approach.

The former of these techniques uses the exact equations of motion to locate stationkeeping locations and the associated necessary ΔV for rendezvous while the latter two techniques employ use of linearized equations of motion.

Using the exact equations of motion (in so far as the two body assumption allows), all identified trajectories for a shuttle-target point rendezvous are integrated. A coordinate system is defined at the target point and is used in the graphical simulation of relative shuttle motion during rendezvous. Comparisons of all identified trajectories are made with respect to fuel consumed, stationkeeping location, total coast time, crew visibility, plume impingement, and general safety.

Conclusions

- (1) Accurate rendezvous trajectories are easily initiated from any stationkeeping location within a 1200 foot radius of

the target point.

- (2) The space shuttle attitude must be continually modified to meet crew visibility constraints during many of the rendezvous trajectories with long coast times.
- (3) One impulse trajectories ($\dot{r}_{FINAL} \leq 0.2$ fps) may be used when approaching bodies to be retrieved to eliminate plume impingement problems.
- (4) One and two impulse solutions were found for the prime stationkeeping point at $X = 1000$ ft. However, all trajectories initiating from the unstable stationkeeping point of $Y = -1000$ ft were two impulse maneuvers.
- (5) Periodic one and two impulse trajectories meeting all imposed constraints were identified for X axis stationkeeping locations.
- (6) Fuel (ΔV) requirements for the line-of-sight approaches were consistently much greater than for the other techniques presented. In some cases, this difference was an order of magnitude.
- (7) Only inplane rendezvous trajectories have been examined, however, similar trajectories are feasible from out-of-plane stationkeeping positions. This is possible because the out-of-plane motion of the shuttle is almost uncoupled from the in-plane motion. Since the two bodies (shuttle and target) are in non-coplanar orbits, their paths will cross twice per orbital revolution. When this occurs, the shuttle may thrust to reduce its velocity component out-of-plane

(relative to the target body) to zero. A standard final rendezvous could then be accomplished. Another alternative would be to project the position of the target body into the orbital plane of the shuttle. A standard rendezvous could then be initiated to this secondary target point. Upon arrival, the \dot{X} and \dot{Y} components would be nullified. Then, a final approach would be made by simply waiting until the two orbits coincided.

Recommendations for Shuttle Proximity Operations

It is recommended that prime stationkeeping locations at $X = \pm 750$ ft be adopted for shuttle proximity operations. The choice between locations ($X = +750$ ft or $X = -750$ ft) is governed by the initial orbital transfer of the shuttle to the stationkeeping location. An elliptical Hohmann transfer from a lower circular orbit to a higher circular orbit will require a velocity increase at the apogee of the ellipse to circularize the orbit. The magnitude of this velocity increase will be great enough to cause plume impingement at distances of 750 ft. Therefore, a stationkeeping point must be selected so that the plume will be expelled away from the target body. This corresponds to locations at $X = +750$ ft. A similar argument may be used to demonstrate that Hohmann transfers from high orbits to lower orbits must aim for stationkeeping locations in front of the target body ($X = -750$ ft) to avoid plume impingement. From either of these points ($X = \pm 750$ ft), a periodic one impulse trajectory may be initiated which results in an approach to within 33 ft of the target point at a relative velocity of 0.2 fps. The benefits of such a rendezvous trajectory are outlined below.

- (1) Total ΔV expended (fuel requirement) is approximately 6% of the amount required for a line-of-sight approach from the same stationkeeping location.
- (2) A constant nose-down shuttle attitude (longitudinal shuttle axis along earth radius vector, nose toward earth) is recommended during rendezvous from $X = + 750$ ft (i.e., from behind the target body). A constant nose-up attitude (longitudinal shuttle axis along earth radius vector, tail towards earth) is suggested for the $X = - 750$ ft stationkeeping location. Such orientations will allow excellent crew visibility during the coast phase and will result in final relative approaches which bring the target body down over the tail and above the cargo bay area. Also, required velocity impulses for rendezvous are efficiently accomplished from this attitude.
- (3) Velocity components in the X direction will be zero at rendezvous initiation as well as at final approach. The magnitude of the initial velocity required is 0.2 fps. This velocity may be achieved by a 37.6 second burn of a single 25 lbf vernier thruster or a 1.08 second burn of one 870 lbf reaction control thruster.
- (4) Since the rendezvous trajectory is a one impulse maneuver, there will be no problem with plume impingement during final approach. However, if it is necessary to completely halt the shuttle, this may safely be done by waiting until the plane of the required RCS thruster has passed the tar-

get body.

- (5) The trajectory is relatively amenable to midcourse corrective impulses to improve the accuracy of approach. To lengthen the trajectory, a \dot{X} velocity component toward the target point is added. To shorten the approach, a \dot{Y} velocity component toward the target point is added. Both thrusts will expell propellant particles away from the target location, thus eliminating all plume impingement considerations.
- (6) The coast time is one-half orbital period, or 2815 seconds for a 250 nm circular orbit. It is envisioned that this time will be spent doing systems checks of the shuttle and the remote manipulator system. Any corrective maneuvers will employ the vernier control system and will not produce excessive forces or bending moments on a fully extended manipulator arm.
- (7) The rendezvous trajectory is periodic with the total period equal to that of the target body around the earth. Thus, if for any reason (satellite tumbling, RMS failure, systems malfunction, etc.) it is decided not to capture the payload, the trajectory may be followed back to the original station-keeping location. If allowed to do so, the shuttle will continue to have a close approach with the target body once during each orbital period. Data from this study indicates that the space shuttle will remain within capture distance of the target for approximately five minutes.

It is also recommended that a series of rendezvous charts be made available to the space shuttle crew. Since the basic contours are the same (nondimensional) for each orbital altitude, a series of transparent overlays could be included for various ranges and closure rates. Also, such charts could prove extremely valuable for use by astronauts involved in extravehicular activities, space tug operations, use of the teleoperator, and for transfer between two orbiting spacecraft, i.e., the shuttle and Skylab. Calculations performed indicate that the error induced by using a rendezvous chart at an altitude other than that for which it was computed is about 8 units per 1000 units of initial range, per 25 nm of orbital altitude difference. For example, an astronaut is 1000 ft from a shuttle which is in a 225 nm circular orbit. If he uses a chart designed for a 250 nm orbit to rendezvous and estimates the necessary velocity components from the charts exactly, he will miss the center of mass of the shuttle by 8 ft (if he started from 1000 meters, he would miss by 8 meters, etc.). If the initial distance was 2000 ft., he would miss by 16 ft. Therefore, it is recommended that rendezvous charts be produced from 100 nm to 500 nm in 50 nm increments for use by the shuttle.

Recommendations for Future Study

The following topics are not within the scope of this thesis yet should be investigated to determine any effects which they may produce on the rendezvous trajectories under consideration for use in the proximity operations phase of a space shuttle mission.

- (1) The incorporation of a revised force model into the analysis which includes such terms as differential drag at low orbital

altitudes and solar radiation pressure at high altitudes is desirable.

(2) The addition of dynamic plume properties to the integration routine is necessary before any definitive conclusions may be drawn about plume forces on the target body during the various rendezvous trajectories.

(3) The effects of errors in assumed stationkeeping location as well as propagation effects of inaccuracies in the first impulse (magnitude or direction) should be more fully evaluated.

In conclusion, all useful trajectories discussed in the text should be further investigated using the Shuttle Engineering Simulator at The Lyndon B. Johnson Spaceflight Center.

REFERENCES

1. Chiu, P. B., et. al., SVDS Plume Impingement Modeling Development, JSC-12976, McDonnell Douglas Technical Services., Houston, Texas, July 1977.
2. Mueller, Donald D., Relative Motion in the Docking Phase of Orbital Rendezvous, AMRL-TDR-62-124, 6570th Aerospace Medical Research Laboratories, Aerospace Medical Division, Wright Patterson Air Force Base, Ohio, November 1962.
3. Dunning, Robert S., The Orbital Mechanics of Flight Mechanics, NASA SP-325, 1975.
4. Higgins, D. B., An Unaided EVA Rendezvous Procedure, Journal of Spacecraft and Rockets, Vol. 14, no. 9, pp. 513-517, 1977.
5. Mueller, Donald D., An Analysis of the Behavior of Long Tether Lines in Space, AMRL-TDR-62-123, 6570th Aerospace Medical Research Laboratories, Aerospace Medical Division, Wright Patterson Air Force Base, Ohio, December 1962.

VITA

Ronald Lafe Farris was born in Austin, Texas on August 2, 1954, the son of Jack D. Farris and Ruth A. Farris. Upon retiring from the Air Force in 1966, Mr. Farris moved his family to Uvalde, Texas where Ron and his older sister Jane graduated from high school. Ron attended the University of Texas at Austin from September 1972 until August 1977, when he received a Bachelor of Science Degree in Aerospace Engineering. As an undergraduate, Ron worked as a student engineer at Bell Helicopter Company in Fort Worth, Texas. This was done through the Co-operative Engineering Program at The University of Texas whereby the student alternates semesters of classwork at UT with semesters of practical engineering experience.

Ron was married to Barbara Kay Burchard of Austin, Texas on January 8, 1977. He officially entered graduate school in September of 1977 and received his Master of Science Degree in Aerospace Engineering in May, 1978.

Permanent Address: Rocksprings Route
Uvalde, TX 78801

, This thesis was typed by Barbara K. Farris.